Taylor & Francis
Taylor & Francis Group

RESEARCH PAPER

OPEN ACCESS   Check for updates

Secretory autophagy machinery and vesicular trafficking are involved in HMGB1 secretion

Young Hun Kim [a,b,c,*], Man Sup Kwak [a,c,*], Bin Lee [a,b], Jae Min Shin [a,b], Sowon Aum [d,e], In Ho Park [c,e], Min Goo Lee [b,d,e], and Jeon-Soo Shin [a,b,c,f]

aDepartment of Microbiology, Yonsei University College of Medicine, Seoul, Korea; bBrain Korea 21 FOUR Project for Medical Science, Yonsei University College of Medicine, Seoul, Korea; cInstitute for Immunology and Immunological Diseases, Yonsei University College of Medicine, Seoul, Korea; dDepartment of Pharmacology, Yonsei University College of Medicine, Seoul, Korea; eSeverance Biomedical Science Institute, Yonsei University College of Medicine, Seoul, Korea; fCenter for Nanomedicine, Institute for Basic Science (IBS), Yonsei University, Seoul, Korea

ABSTRACT

Nuclear protein HMGB1 is secreted in response to various stimuli and functions as a danger-associated molecular pattern. Extracellular HMGB1 induces inflammation, cytokine production, and immune cell recruitment via activation of various receptors. As HMGB1 does not contain an endoplasmic reticulum-targeting signal peptide, HMGB1 is secreted via the endoplasmic reticulum-Golgi independently via an unconventional secretion pathway. However, the mechanism underlying HMGB1 secretion remains largely unknown. Here, we investigated the role of secretory autophagy machinery and vesicular trafficking in HMGB1 secretion. We observed that HSP90AA1 (heat shock protein 90 alpha family class A member 1), a stress-inducible protein, regulates the translocation of HMGB1 from the nucleus to the cytoplasm and its secretion through direct interaction. Additionally, geldanamycin, an HSP90AA1 inhibitor, reduced HMGB1 secretion. GORASP2/GRASP55 (golgi reassembly stacking protein 2), ARF1^{Q71L} (ADP ribosylation factor 1), and SAR1A^{T39N} (secretion associated Ras related GTPase 1A), which promoted unconventional protein secretion, increased HMGB1 secretion. HMGB1 secretion was inhibited by an early autophagy inhibitor and diminished in ATG5-deficient cells even when GORASP2 was overexpressed. In contrast, a late autophagy inhibitor increased HMGB1 secretion under the same conditions. The multivesicular body formation inhibitor GW4869 dramatically decreased HMGB1 secretion under HMGB1 secretion-inducing conditions. Thus, we demonstrated that secretory autophagy and multivesicular body formation mediate HMGB1 secretion.

Introduction

HMGB1 (high mobility group box 1), identified as a non-histone nuclear protein, is a DNA chaperone that repairs and stabilizes the chromatin structure [1,2]. HMGB1 plays important roles in macroautophagy/autophagy and metabolism and is secreted into the extracellular fluid in response to various stimuli, where it acts as a danger-associated molecular pattern to induce sterile inflammation and cell migration [3,4]. In HMGB1 secretion, which is inflammasome-mediated and involves an autophagy-regulated mechanism, post-translational modifications of acetylation, phosphorylation, and N-linked glycosylation are involved [5–13]. HMGB1 translocation from the nucleus to the cytoplasm is regulated by the nuclear export protein XPO1/CRM1 [8]. However, the specific molecular mechanism of HMGB1 secretion is unknown.

Most eukaryotic proteins are secreted through the conventional endoplasmic reticulum (ER)-Golgi secretory pathway. These proteins contain signal peptides for being targeted into the ER. However, some proteins are secreted via an ER-Golgi

independent pathway known as unconventional protein secretion (UCPS). Unconventionally secreted proteins are generally involved in immune surveillance, cell survival, and cellular stress [14]. In addition, the UCPS pathway includes various mechanisms. Type I secretion involves the direct, pore-mediated translocation of a cytoplasmic protein across the plasma membrane without the formation of vesicular intermediates. The most well-studied protein that uses this type of secretion is FGF2 (fibroblast growth factor 2). Membrane translocation of this protein is promoted by a self-sustained mechanism driven by PtdIns(4,5)P$_2$-dependent oligomerization [15]. Type II secretion systems involve ABC transporters, which are used to translocate lipidated peptides and proteins. Type III secretion involves autophagosome/endosome-based secretion mediated by intracellular vesicles, such as secretory lysosomes, microvesicles, and multivesicular bodies (MVBs). The secretion of IL1B/IL-1β (interleukin 1 beta) is one of the most widely studied examples of type III secretion. IL1B secretion depends on CASP1 (caspase 1)-dependent proteolytic cleavage mediated by intracellular inflammasome

---

activation [16]. Recently, ATG5 (autophagy related 5), the small GTPase RAB8A, and GORASP2/GRASP55 (golgi reassembly stacking protein 2) were found to be involved in IL1B secretion [17]. Type IV secretion systems, for the Golgi-bypass secretion of plasma membrane resident proteins, use a classical secretory pathway. The secretion of transmembrane proteins involves anterograde transport from the ER to the plasma membrane without passage through the Golgi complex [14,18,19].

Autophagy is a process that mediates the clearance of cellular components, such as lipids, aggregated proteins, and damaged organelles, which are recycled to maintain cellular homeostasis. Autophagy not only functions in protein degradation but also protein secretion. The autophagy-mediated protein secretion mechanism is known as secretory autophagy. This mechanism is not well-understood; however, it reportedly differs from degradative autophagy-based on the participation of specific proteins, Grh1 (yeast ortholog of the mammalian Golgi reassembly stacking protein 1), Bug1, and endosomal sorting complexes required for transport (ESCRT)-II and -III proteins for the biogenesis of the compartment of UCPS in yeast. The GORASP family (GORASP1/GRASP65 and GORASP2/GRASP55) is crucial for the unconventional secretion of cytoplasmic proteins and Golgi-bypass proteins [20]. GORASP proteins are found on the stacks of Golgi cisternae and function to tether vesicles for fusion with the Golgi apparatus. GORASPs depletion appears to impair protein trafficking and disrupt the Golgi structure [21]. Moreover, GORASP proteins induce the formation of the compartment of UCPS in yeast and promote IL1B secretion from macrophages [17,19].

As a stress-inducible protein, HSP90AA1 (heat shock protein 90 alpha family class A member 1) functions as a protein chaperone of misfolded proteins to maintain cell homeostasis. HSP90AA1 regulates the stability and activity of protein kinases, transcription factors, and cell signaling proteins under normal and stress conditions [22,23]. Additionally, HSP90AA1 regulates UCPS of IL1B by facilitating the entry of IL1B into vesicles [24].

In this study, we investigated the role of HSP90AA1 in the nucleo-cytoplasmic shuttling and secretion of HMGB1. To the best of our knowledge, this is the first report indicating that HMGB1 could bind to HSP90AA1. Our data demonstrate that secretory autophagy machinery and vesicular trafficking components participate in the unconventional secretion of HMGB1 using GORASP2, SAR1A^{T39N}, and ARF1^{Q71L} and MVB formation.

Results

HSP90AA1 binds to HMGB1, resulting in its secretion

The function of HMGB1 is altered when it interacts with specific binding partners [25]. To search for novel binding partners of HMGB1, human embryonic kidney (HEK) 293 T cells were first transfected with *MYC/cMyc-HMGB1*, and then whole-cell lysates (WCLs) were pulled-down using MYC affinity beads. HMGB1-binding molecules, including HSP90AA1, were analyzed by mass spectrometry (**Fig. S1A**). HSP90AA1 was found to interact with HMGB1 through exogenous transfection analysis using immunoprecipitation (IP) and proximity ligation assay (PLA) (Figure 1A **and S1B**). The endogenous binding of HMGB1 to HSP90AA1 was detected under starvation conditions in Earle's balanced salt solution (EBSS) by IP and PLA (Figure 1B and 1C). The interaction between HMGB1 and HSP90AA1 was mostly observed in the nucleus. Subdomain analysis of HSP90AA1 showed that HMGB1 was bound to both the HSP90AA1 N-terminal domain (NTD) and the middle domain (MD) but not the C-terminal domain (CTD) (Figure 1D **and S1C**). In contrast, HSP90AA1 interacted with wild type (WT) HMGB1 and the C-tail deletion mutant (ΔC) (Figure 1E **and S1C**). We observed a direct interaction between HMGB1 and HSP90AA1 by enzyme-linked immunosorbent assay (ELISA) and *in vitro* binding assay (Figure 1F **and S1D**).

Nuclear HSPA7/HSP70/HSP72, another HSP family protein, suppresses HMGB1 nucleo-cytoplasmic translocation under oxidative stress or mild heat shock conditions [26]. When HEK293T cells were co-transfected with *HMGB1-GFP* and *HSP90AA1-Flag*, HMGB1 was mostly localized in the cytoplasm, regardless of whether starvation stress was present or absent; this localization was inhibited by geldanamycin (GA), an HSP90AA1 inhibitor (Figure 2A). Previously, we demonstrated that oxidation of HMGB1 to form an intramolecular disulfide bond between C23 and C45 is a prerequisite for its nucleo-cytoplasmic translocation [27]. The HMGB1^{C23S} mutant, however, was observed in the nucleus upon HSP90AA1 overexpression (**Fig. S2A**), although the interaction between HSP90AA1 and HMGB1^{C23S} was similar to that with WT HMGB1 (**Fig. S2B**). These data indicate that HSP90AA1 binds to HMGB1 in the nucleus and facilitates its nucleo-cytoplasmic translocation.

Overexpression of the HSP90AA1 NTD and MD induced cytoplasmic translocation of HMGB1 in HEK293T cells (Figure 2B). HMGB1 secretion was increased by HSP90AA1 overexpression and decreased by *HSP90AA1* knockdown or GA treatment under starvation conditions (Figure 2(C-E)). The phosphorylation and acetylation of HMGB1 caused by phorbol 12-myristate 13-acetate (PMA) and trichostatin A (TSA) treatments, respectively, induce HMGB1 secretion [7,8]. These effects were inhibited by GA (**Fig. S2C**), indicating that HSP90AA1 is important for HMGB1 translocation and secretion.

HSP90AA1 increases the binding of HMGB1 to XPO1

HSP90AA1 promotes the cytoplasmic translocation of MTA1 (metastasis associated 1) along with the nuclear export protein XPO1 [28]. HSP90AA1 interacts with XPO1 to facilitate its nucleo-cytoplasmic translocation [29]. Cytoplasmic translocation of HMGB1 is mediated by XPO1 [8]. We hypothesized that HSP90AA1 increased the interaction between HMGB1 and XPO1. HSP90AA1 overexpression increased the binding of HMGB1 to XPO1 (Figure 2C), and the HSP90AA1 NTD and MD increased the binding between HMGB1 and XPO1 (Figure 3A). The specific binding and the nucleo-cytoplasmic translocation of HMGB1 were inhibited by leptomycin B (LMB), a XPO1 inhibitor (Figure 3(B,C)). These results
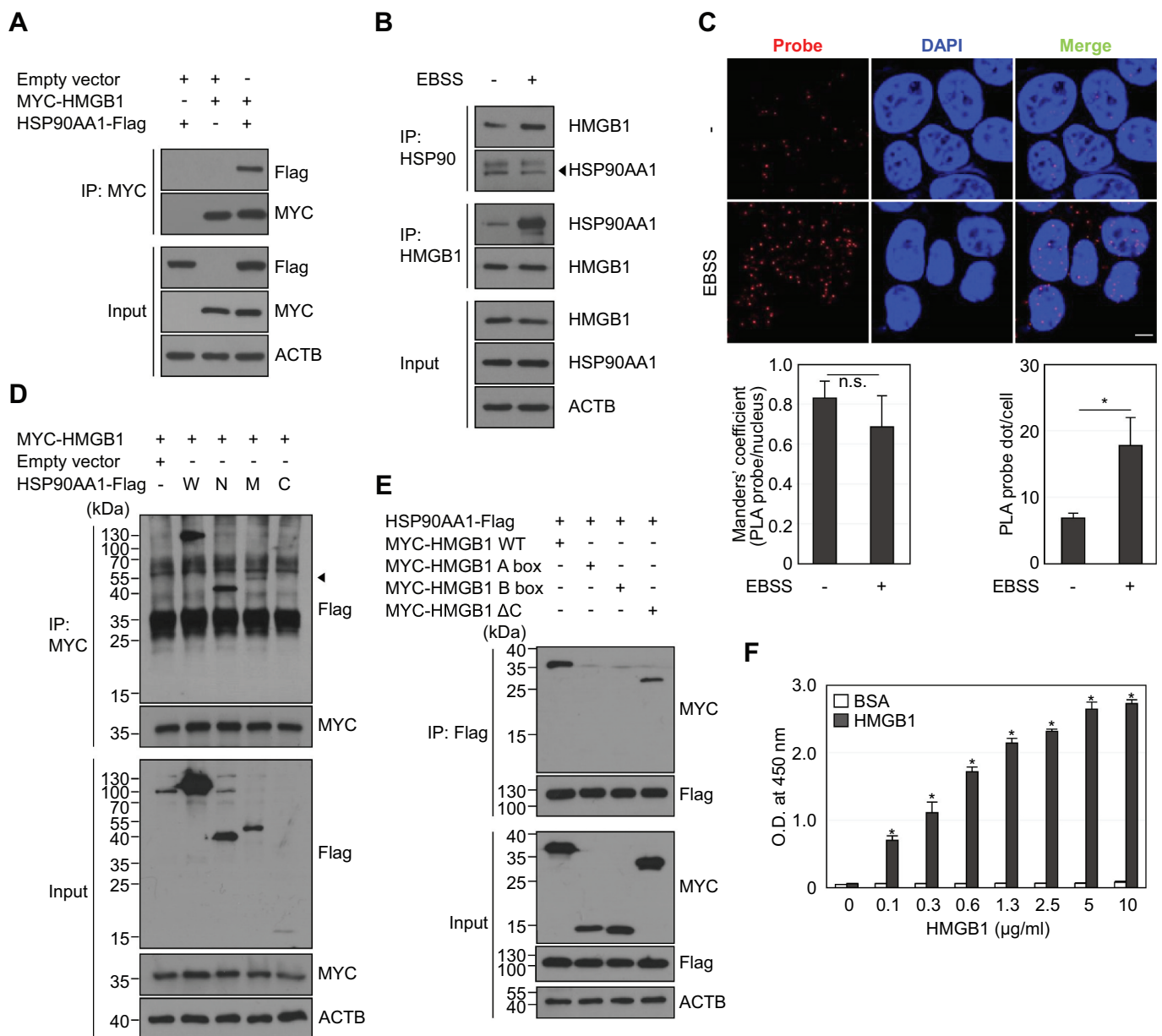
Figure 1. HSP90AA1 interacts with HMGB1. (A) HEK293T cells were co-transfected with *MYC-HMGB1* and *HSP90AA1-Flag* and incubated for 48 h. WCLs were immunoprecipitated (IP) against MYC, and immunoblotted (IB) with anti-Flag, anti-MYC, and anti-ACTB antibodies. (B) The cells were treated with EBSS for 6 h. WCLs were immunoprecipitated with anti-HSP90 and anti-HMGB1 antibodies and immunoblotted with anti-HMGB1 and anti-HSP90, and anti-ACTB antibodies. (C) HEK293T cells were treated with EBSS for 6 h, and the interaction between HMGB1 and HSP90AA1 was observed using PLA. Scale bar: 5 μm. (D, E) To observe the interactions between HMGB1 (Boxes A and B, and ΔC-HMGB1) and HSP90AA1 domains [W (Wild type), N (N-terminal domain), M (middle domain), and C (C-terminal domain)-Flag], HEK293T cells were transfected for 48 h, and WCLs were immunoprecipitated and immunoblotted. Arrowhead: HSP90AA1 MD. (F) Recombinant HSP90AA1 was coated on the polystyrene microplate for 18 h, and serially diluted recombinant HMGB1 was added for 1 h for ELISA. BSA was used as a control protein. Data are presented as the mean ± SEM from at least three independent experiments. n.s.: not significant, *$p < 0.001$, compared to each control, two-tailed unpaired Student's *t*-test with equal variances.

indicate that HSP90AA1 promotes the interaction between HMGB1 and XPO1 for cytoplasmic translocation of HMGB1.

GORASP2 increases HMGB1 secretion

The GORASP2-dependent autophagy machinery plays a vital role in the secretion of leaderless proteins, such as IL1B [17]. We thus next investigated the secretory autophagy machinery involved in HMGB1 secretion. GORASP has two isoforms: GORASP1 and GORASP2. GORASP1 is involved in the early stage of ER to Golgi transport, and GORASP2 is sensitive to

cargo-related transport [30]. Thus, we focused on the role of GORASP2 in HMGB1 secretion. When GORASP2 was overexpressed in HEK293T cells, HMGB1 secretion was augmented by starvation and PMA- and TSA-treated conditions (Figure 4A and S3A), and knockdown of *GORASP2* reduced HMGB1 secretion (Figure 4B). We next evaluated how GORASP2 increases HMGB1 secretion. GORASP2 showed no binding to HMGB1 in our study (**Fig. S3B**), but GORASP2 overexpression induced the cytoplasmic localization of HMGB1 (**Fig. S3C**), suggesting an indirect effect of GORASP2 on HMGB1
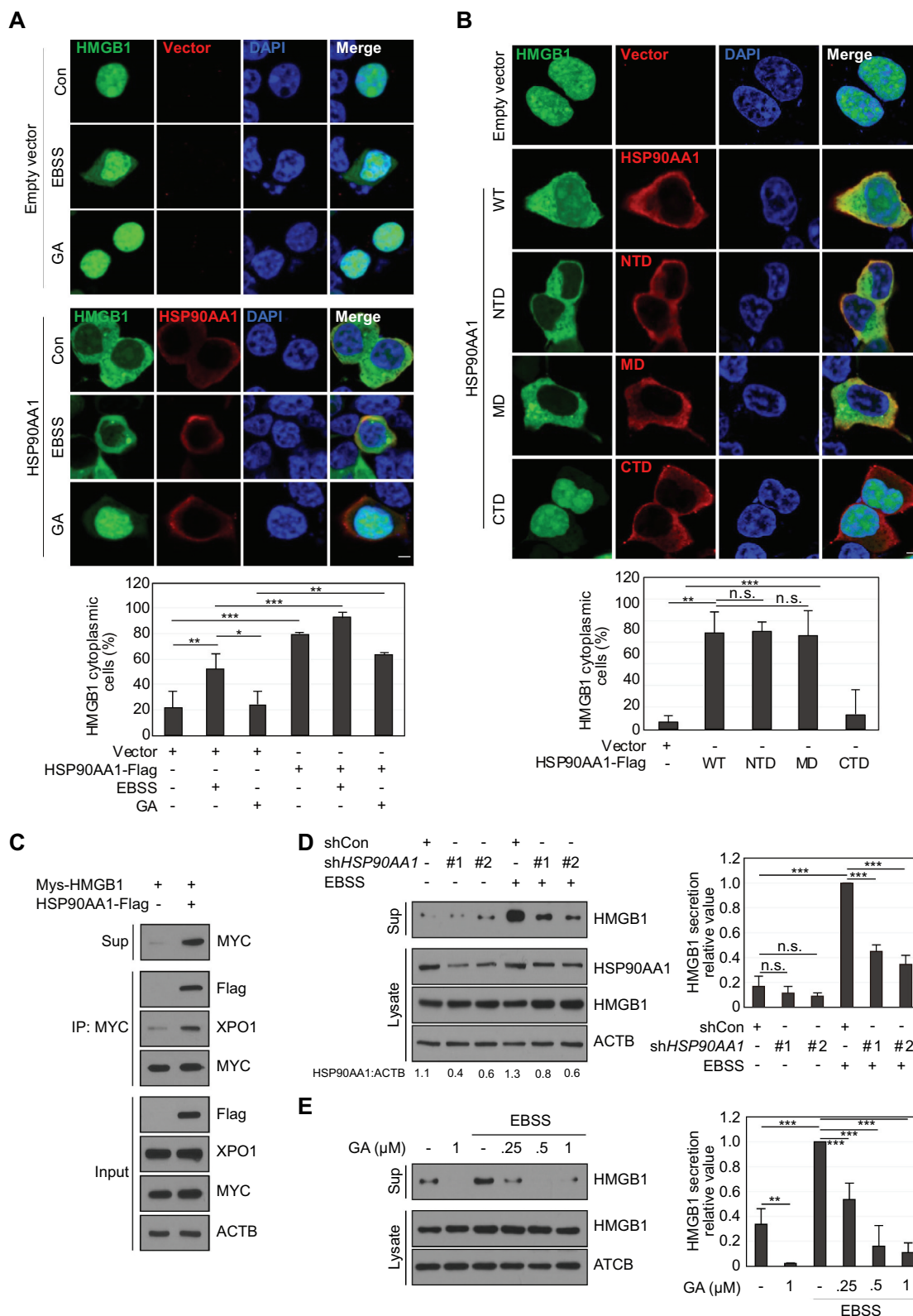
Figure 2. HSP90AA1 increases HMGB1 secretion by promoting HMGB1 cytoplasmic translocation. (A, B) HEK293T cells were co-transfected with *HMGB1-GFP* and *HSP90AA1-Flag* or *HMGB1-GFP* and *HSP90AA1 WT, NTD, MD,* or *CTD-Flag*. After 48 h, the cells were treated with 0.5 μM geldanamycin (GA) and EBSS for 6 h. The cells were immunostained with anti-Flag antibody (red). Subcellular localization of HMGB1 was observed using a confocal microscope. Scale bar: 5 μm. The number of cytoplasmic HMGB1-positive cells was counted among over 200 GFP-positive cells. (C) *MYC-HMGB1* and *HSP90AA1-Flag* were transfected into HEK293T cells. WCLs were performed IP using anti-MYC antibody and immunoblotting with anti-MYC, anti-Flag, anti-XPO1, and anti-ACTB antibodies. The culture supernatants were concentrated with Amicon Centricon filters. (D) HEK293T cells were transiently transfected with shRNA control (SHC001) or sh*HSP90AA1* (#1; TRCN0000315007 and #2; TRCN0000315009). After 48 h, the cells were incubated in EBSS for 14 h. Immunoblotting was performed as indicated. (E) HEK293T cells were pretreated with dose-dependently GA treatment for 2 h. The cells were incubated in EBSS media for 14 h. WCLs were immunoblotted with anti-HMGB1 and anti-ACTB antibodies. The culture supernatants were concentrated with Amicon Centricon filters. Data are presented as the mean ± SEM from at least three independent experiments. n.s.: not significant, *$p < 0.05$, **$p < 0.01$, ***$p < 0.001$, one-way ANOVA analysis of variance followed by Tukey honestly significant difference posthoc test for multiple comparisons.

Figure 3. XPO1 influences HSP90AA1-mediated HMGB1 cytoplasmic translocation. (A) *MYC-HMGB1* and *HSP90AA1 W* (Wild type), *N* (N-terminal domain), *M* (middle domain), and *C* (C-terminal domain)-*Flag* were transfected into HEK2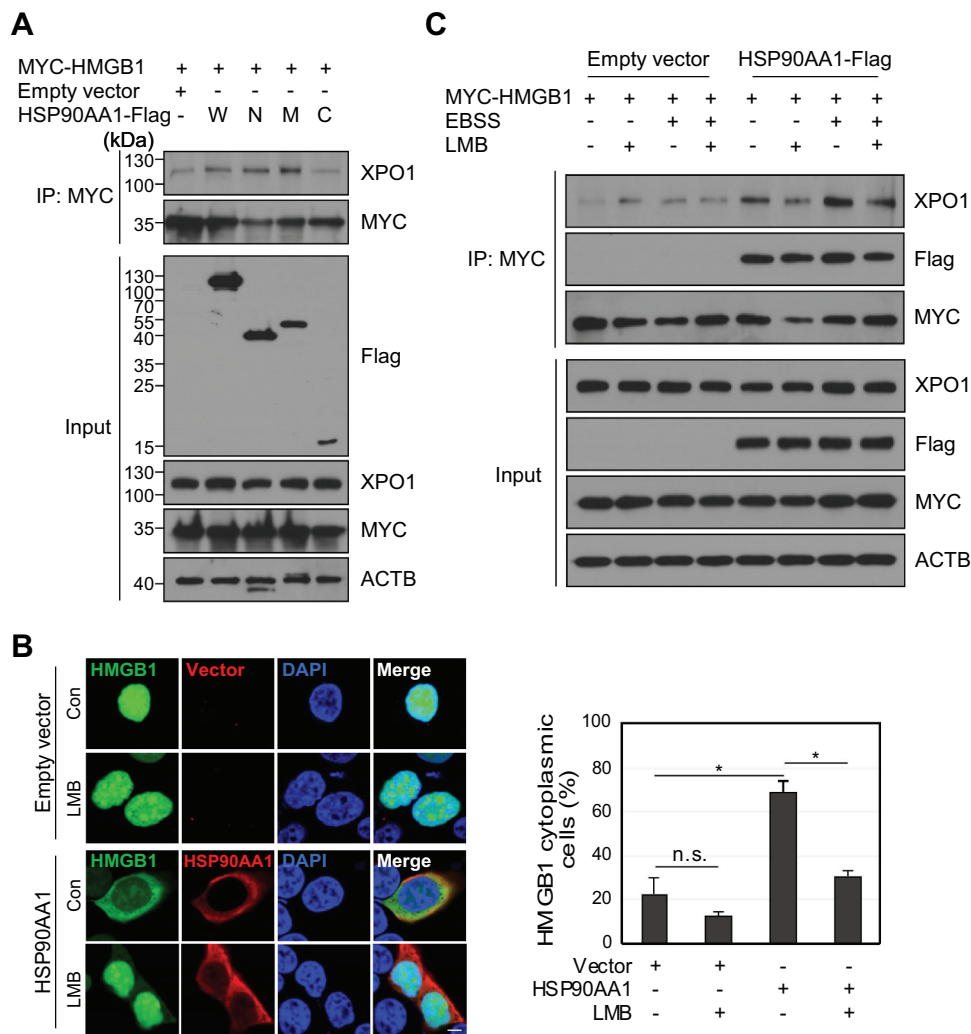93T cells. WCLs were evaluated by IP using anti-MYC antibody and immunoblotted using anti-MYC, anti-Flag, anti-XPO1, and anti-ACTB antibodies. Culture supernatants were concentrated with Amicon Centricon filters. (B) HEK293T cells were transfected with *HMGB1-GFP* and *HSP90AA1-Flag* for 24 h and then treated with 20 ng/mL LMB for 24 h. The cells were immunostained with anti-Flag antibody (red). The localization of HMGB1 was observed using a confocal microscope. Scale bar: 5 μm. The number of cytoplasmic HMGB1-positive cells was counted among over 200 GFP-positive cells. n.s.: not significant, *$p < 0.001$. (C) HEK293T cells were transfected with *MYC-HMGB1* and *HSP90AA1-Flag*. The cells were pretreated with 30 ng/mL LMB for 1 h and incubated in EBSS media for 6 h. WCLs were immunoprecipitated with anti-MYC antibody and immunoblotted with anti-XPO1, anti-Flag, anti-MYC, and anti-ACTB antibodies.

secretion. PRDX2 (peroxiredoxin 2) was used as a positive control molecule for HMGB1 binding [27].

We tested the interaction between HSP90AA1 and GORASP2 using IP to confirm the correlation between HSP90AA1 and GORASP2 because both HSP90AA1 and GORASP2 increased HMGB1 secretion according to our previous results. However, no direct interaction was observed (**Fig. S3D**). HMGB1 secretion, however, showed a greater increase when both HSP90AA1 and GORASP2 were exogenously co-expressed and decreased by GA treatment (Figure 4(C,D)). Thus, HSP90AA1 and GORASP2 synergistically promoted HMGB1 secretion.

The autophagy machinery regulates HSP90AA1 and GORASP2-mediated HMGB1 secretion

HMGB1 secretion is related to secretory autophagy [6,17,31], and both HSP90AA1 and GORASP2 are related to autophagy formation [17,32]. We tested the autophagy machinery induced by HSP90AA1 and GORASP2 for HMGB1 secretion. Autophagosome formation was increased by GORASP2 over-expression and decreased by GA treatment in the presence of chloroquine (CQ) (**Fig. S4A and S4B**), suggesting that HSP90AA1 and GORASP2 induce autophagy flux. Colocalization of HMGB1 and MAP1LC3/LC3 (microtubule-associated protein 1 light chain) was increased by either HSP90AA1 or GORASP2 overexpression according to confocal microscopy analysis and IP assay (Figure 5(A-C) and S4C). These results indicate that both HSP90AA1 and GORASP2 increase autophagy flux and promote HMGB1 and LC3 coloca-lization. HMGB1 secretion was inhibited by the early autophagy inhibitor wortmannin (Wort) but promoted by the late autophagy inhibitors Baf and CQ [33] under starvation or PMA treat-ment (Figure 5(D,E), and S4D); the increase in secretion was decreased by GA treatment (Figure 5E and S4E).
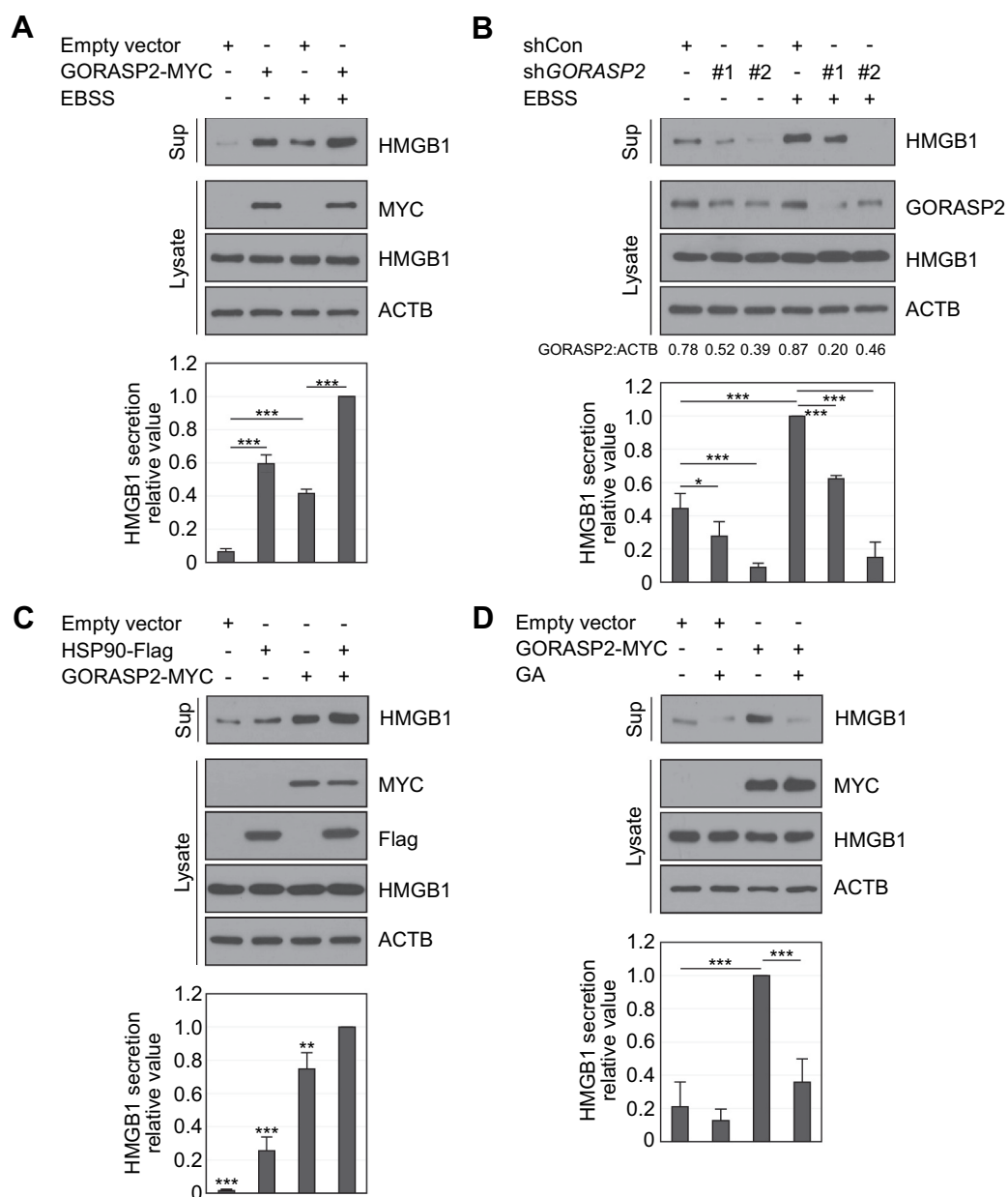
Figure 4. GORASP2 increases HMGB1 secretion. (A, B) HEK293T cells were transfected with *GORASP2-MYC*, shRNA control (SHC001) or sh*GORASP2* (#1; TRCN0000129348 and #2; TRCN0000127611). The cells were incubated in EBSS media for 14 h. WCLs were immunoblotted with anti-MYC, anti-HMGB1, anti-GORASP2, and anti-ACTB antibodies. The culture supernatants were concentrated with Amicon Centricon filters. (C) *GORASP2-MYC* and *HSP90AA1-Flag* were transfected into HEK293T cells. WCLs were immunoblotted with anti-MYC, anti-Flag, anti-HMGB1, and anti-ACTB antibodies. Culture supernatants were concentrated with Centricon filters. Results were compared to those for co-expressed HSP90AA1 and GORASP2/GRASP55. (D) *GORASP2-MYC* was transfected and treated with 0.5 μM GA for 24 h. WCLs were immunoblotted with anti-MYC, anti-HMGB1, and anti-ACTB antibodies. Culture supernatants were concentrated with Centricon filters. Data are presented as the mean ± SEM from at least three independent experiments. *$p < 0.05$, **$p < 0.01$, ***$p < 0.001$, one-way ANOVA followed by Tukey honestly significant difference posthoc test for multiple comparisons.

HMGB1 secretion was detected in WT mouse embryonic fibroblasts (MEFs) under CQ treatment or starvation conditions but dramatically decreased in *atg5*$^{-/-}$ MEF cells (**Fig. S4F and S4G**). GORASP2 overexpression also showed no influence of HMGB1 secretion in *atg5*$^{-/-}$ MEF cells (Figure 5F). These results suggest that HMGB1 secretion is regulated by both HSP90AA1- and GORASP2-mediated secretory autophagy machinery involving autophagosome formation and maturation but not by autophagosome-lysosome fusion.

Next, we tested whether HMGB1 secretion requires extracellular vesicle (EV) loading during GORASP2-autophagy-mediated secretion. Culture supernatants were collected from WT MEF and *atg5*$^{-/-}$ MEF cells (Figure 5G) and WT mouse bone marrow-derived macrophages (BMDM) and *gorasp2*$^{-/-}$ BMDM after EBSS or LPS treatment (**Fig. S5A**). After separating EVs from the culture supernatant by a differential ultracentrifugation series, EVs were exposed to proteinase K with or without Triton X-100 to observe HMGB1 loading in EVs. Proteinase K is expected to digest HMGB1 in the presence of Triton X-100,
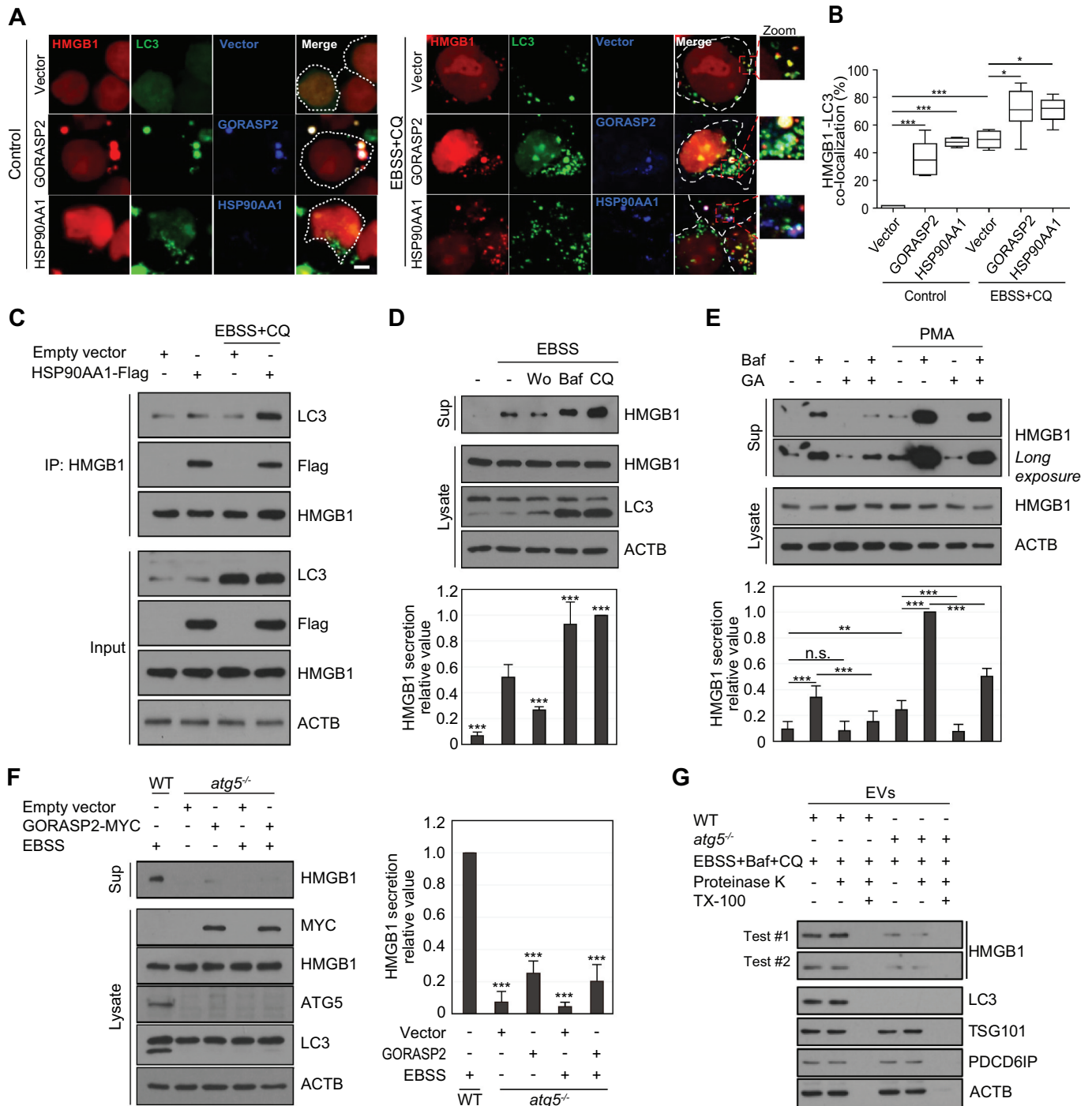
Figure 5. Autophagy machinery regulates HSP90AA1 and GORASP2-mediated HMGB1 secretion. (A) HEK293T cells were transfected with *HMGB1-mCherry, GFP-LC3, GORASP2-MYC*, and *HSP90AA1-Flag* for 48 h, and treated with 20 μM CQ under EBSS treatment for 4 h. The cells were permeabilized with 20 μg/mL digitonin buffer in PBS on ice for 5 min. The cells were immunostained with anti-Flag and anti-MYC antibodies. (B) Quantification analysis of co-localization of HMGB1 and LC3. Scale bar: 5 μm. (C) HEK293T cells were transfected with *HSP90AA1-Flag* and treated with 20 μM CQ under EBSS treatment for 4 h. WCLs were immunoprecipitated with anti-HMGB1 antibody and immunoblotted with anti-LC3, anti-Flag, anti-HMGB1, and anti-ACTB antibodies. (D) HEK293T were pretreated with 100 nM wortmannin (Wo), 20 nM bafilomycin A1 (Baf), and 20 μM chloroquine (CQ) for 2 h and incubated in EBSS media for 14 h. WCLs were immunoblotted with anti-HMGB1, anti-LC3, and anti-ACTB antibodies. Culture supernatants were concentrated with Centricon filters. All results were compared to EBSS treatment alone. (E) The cells were pretreated with 0.5 μM GA for 2 h and then treated with 20 nM Baf and 350 nM PMA for 24 h. Immunoblotting was performed against anti-HMGB1 and anti-ACTB antibodies. (F) ATG5-inducible Tet-off MEF cells were cultured in presence and absence 1 μg/mL doxycycline for 48 h to generate *atg5* knockout (*atg5⁻/⁻* MEF) cells. *atg5* knockout cells were transfected with *GORASP2-MYC*. The cells were incubated in EBSS media for 14 h. WCLs were immunoblotted with anti-HMGB1, anti-LC3, anti-ATG5, anti-MYC, and anti-ACTB antibodies. The culture supernatants were concentrated with Centricon filters. Results were compared to those obtained using WT MEF cells. (G) EVs of WT MEF and *atg5⁻/⁻* MEF cells were treated with 20 μg/mL proteinase K with or without 1% Triton X-100 (TX-100) for 1 h at 37°C, and HMGB1 protection in EVs was evaluated by immunoblotting. EVs were immunoblotted with anti-HMGB1, anti-LC3, anti-TSG101, anti-PDCD6IP/Alix, and anti-ACTB antibodies. (A-F) Data are presented as the mean ± SEM from at least three independent experiments. n.s.: not significant, *$p < 0.05$, **$p < 0.01$, ***$p < 0.001$, one-way ANOVA followed by Tukey honestly significant difference posthoc test for multiple comparisons.
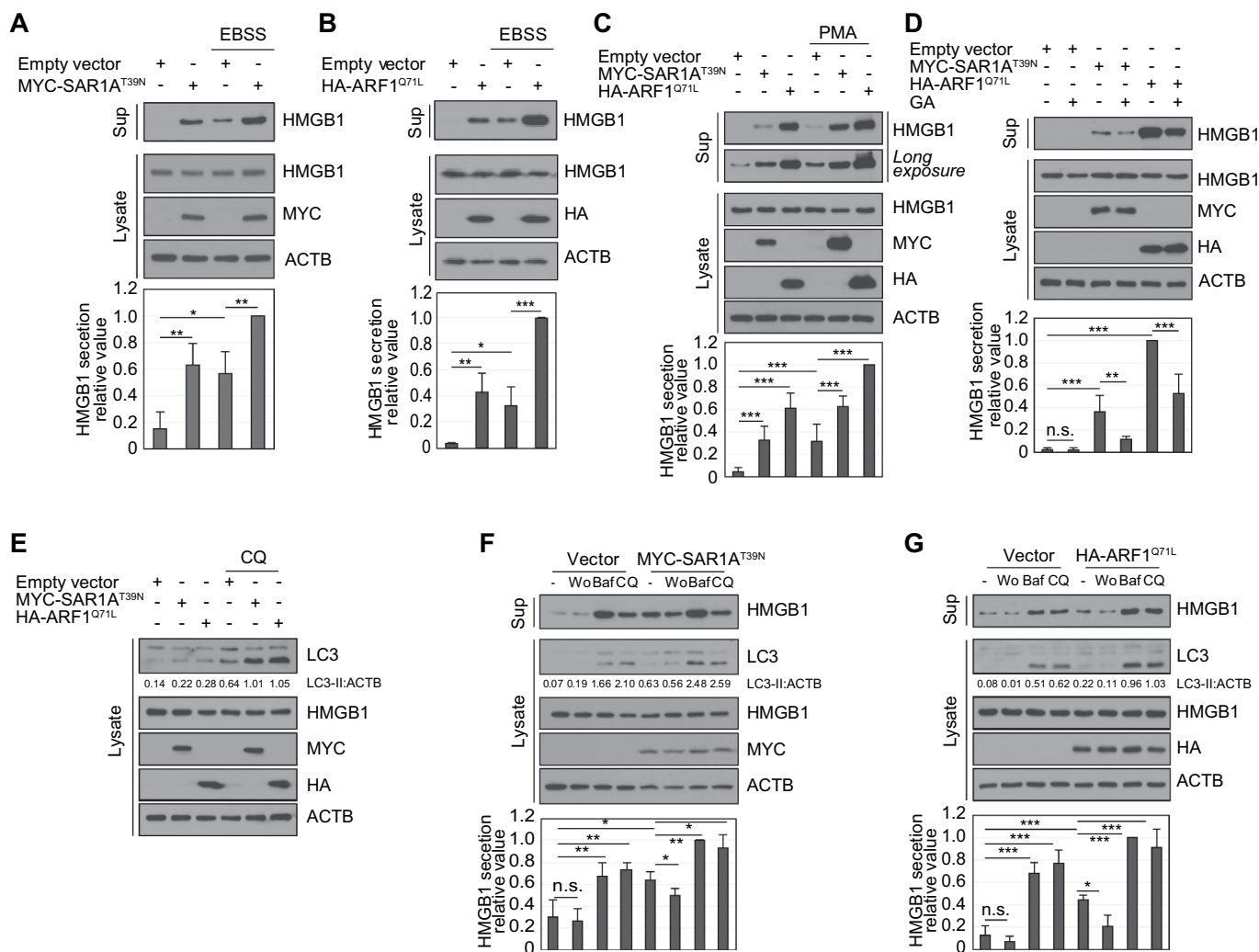
Figure 6. Small G protein SAR1A and ARF1 dominant-negative mutants participate in HMGB1 secretion by promoting secretory autophagy-mediated secretion pathway. (A-D) HEK293T cells were transfected with *MYC-SAR1A^T39N^* and *HA-ARF1^Q71L^*. The cells incubated in EBSS for 14 h (A, B), 350 nM PMA (C), and 0.5 μM GA (D) for 24 h. WCLs and culture medium were evaluated using anti-HMGB1, anti-MYC, anti-HA, and anti-ACTB antibodies. (E) HEK293T cells were transiently transfected with *MYC-SAR1A^T39N^* and *HA-ARF1^Q71L^* and treated with 20 μM CQ for 24 h. WCLs were examined by immunoblotting against anti-LC3, anti-HMGB1, anti-MYC, anti-HA, and anti-ACTB antibodies. (F, G) HEK293T transfected with *MYC-SAR1A^T39N^* (F), and *HA-ARF1^Q71L^* (G) were treated with 100 nM Wo, 20 nM Baf, and 20 μM CQ for 24 h. WCLs and culture supernatants were evaluated by immunoblotting against anti-LC3, anti-HMGB1, anti-MYC, anti-HA, and anti-ACTB antibodies. Data are presented as the mean ± SEM from at least three independent experiments. n.s.: not significant, *$p < 0.05$, **$p < 0.01$, ***$p < 0.001$, one-way ANOVA followed by Tukey honestly significant difference posthoc test for multiple comparisons.

which releases HMGB1 from EVs through disintegrating the membrane. HMGB1 could be detected in proteinase K-treated EVs from WT MEF cells and WT BMDM cells in the absence of Triton X-100 and was not nearly detected in the presence of Triton X-100, indicating that HMGB1 was present inside EVs (Figure 5G **and S5A**). The levels of HMGB1 loading in EVs of *atg5*^−/−^ MEF cells and *gorasp2*^−/−^ BMDM were significantly reduced compared to those in WT MEF cells and WT BMDM cells, respectively (Figure 5G **and S5A**). These results indicate that GORASP2- and autophagy-mediated HMGB1 secretion play a vital role in EV loading.

A recent study suggested that autophagy-mediated unconventional secretion via EVs requires LC3 conjugation machinery, such as ATG7 and ATG12, called "LC3-dependent EV loading and secretion (LDELS)" [34]. In our study, HMGB1 secretion was reduced in the knockdowns of LC3 conjugation elements, namely *ATG7* and *ATG12*, in starvation conditions

(**Fig. S5B and S5C**). ATG14 plays a vital role in the initiation process of BECN1 (beclin 1) and phosphatidylinositol-3 kinase (PtdIns3K) complex-associated autophagy [35]. Besides, HMGB1 secretion was decreased in *ATG14* knockdown cells and *atg14*^−/−^ HCT116 cells under the EBSS condition (**Fig. S5D and S5E**). Moreover, we observed that HMGB1 secretion was inhibited by the early autophagy inhibitor of Wort upon either EBSS or PMA treatment (Figure 5D **and S4D**). These results indicate that autophagy-mediated HMGB1 secretion is dependent on the initiation and LC3 conjugation steps during autophagy execution.

SAR1A and ARF1 dominant-negative mutants enhance HMGB1 secretion via secretory autophagy pathway

SAR1A (secretion-associated Ras-related GTPase 1A) and ARF1 (ADP ribosylation factor 1), which are components of
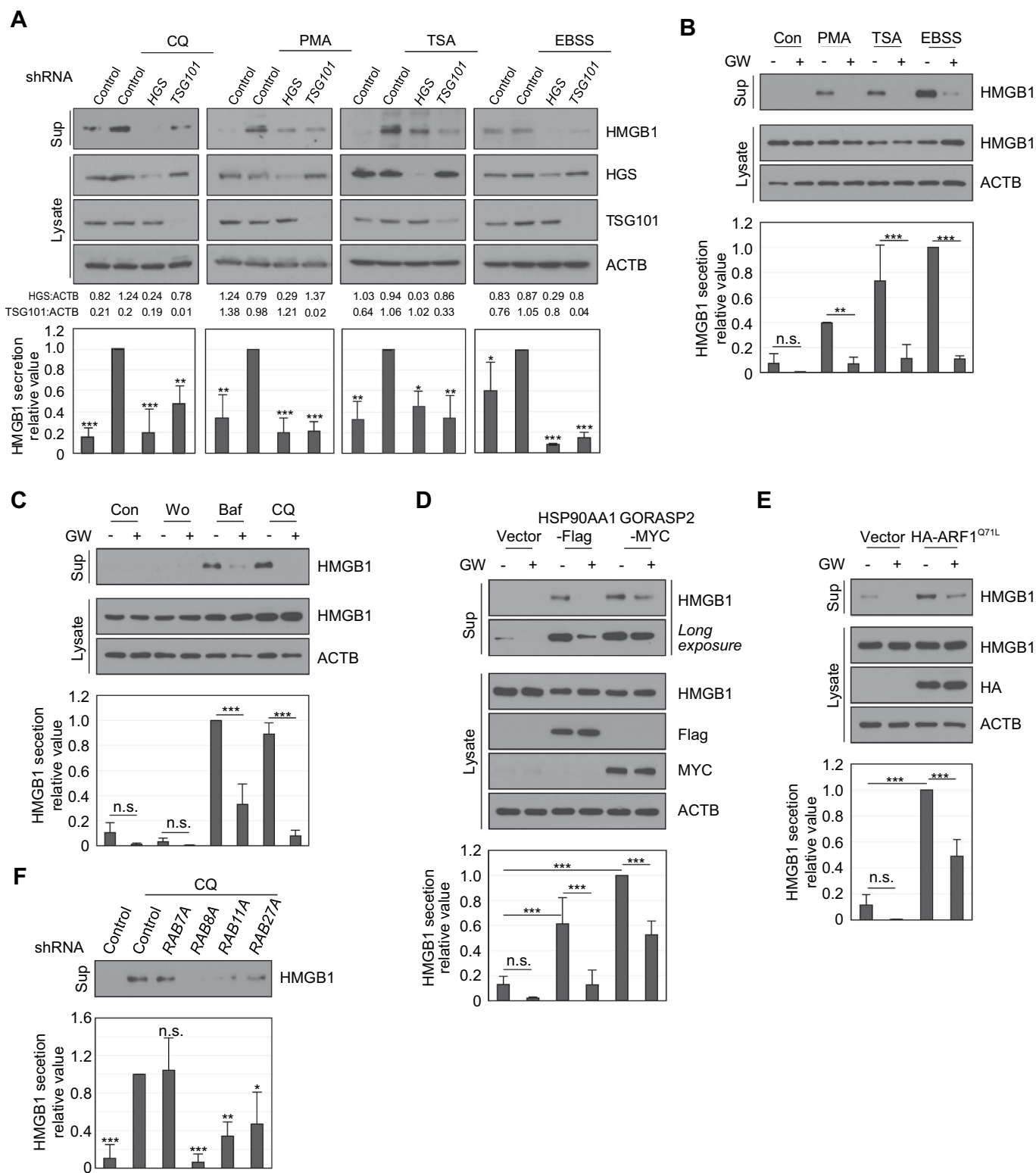
Figure 7. MVB formation is crucial in HMGB1 secretion. (A) HEK293T cells were transiently transfected with shRNA control (SHC001), sh*HGS* (TRCN0000379833), and sh*TSG101* (TRCN0000315042) for 24 h. The cells were treated with 20 μM CQ, 350 nM PMA, and 25 ng/mL TSA for 24 h and with EBSS for 14 h. Culture supernatants and WCLs were immunoblotted with anti-HMGB1, anti-HGS, anti-TSG101, and anti-ACTB antibodies. All results were compared to that for the shRNA control for each treatment. (B, C) HEK293T cells pretreated with 2 μM GW4869 for 2 h, and treated with 350 nM PMA and 25 ng/mL TSA for 24 h, and EBSS for 14 h (B); 100 nM Wo, 20 nM Baf, and 20 μM CQ for 24 h (C). WCLs and supernatants were immunoblotted with anti-HMGB1 and anti-ACTB antibodies. (D, E) HEK293T cells were transfected with *HSP90AA1-Flag* and *GORASP2-MYC* (D); *HA-ARF1^{Q71L}* (E) for 24 h. The cells were treated with 2 μM GW4869 for 24 h. Culture supernatants and WCLs were immunoblotted with anti-HMGB1, anti-HA, and anti-ACTB antibodies. (F) HEK293T cells were transiently transfected with shRNA control, sh*RAB7A* (TRCN0000229643), sh*RAB8A* (TRCN0000048216), sh*RAB11* (TRCN0000073021), and sh*RAB27A* (TRCN0000005295) for 24 h. The cells were treated with 20 μM CQ for 24 h. Culture supernatants were immunoblotted with anti-HMGB1 antibodies. All results were compared to those of the shRNA control treated with CQ. Data are presented as the mean ± SEM from at least three independent experiments. n.s.: not significant, $*p < 0.05$, $**p < 0.01$, $***p < 0.001$, one-way ANOVA followed by Tukey honestly significant difference posthoc test for multiple comparisons.

Figure 8. HMGB1 secretion is regulated by autophagy-mediated secretion in macrophages. (A) RAW264.7 cells were pretreated with 100 nM Wo, 20 nM Baf, 20 μM CQ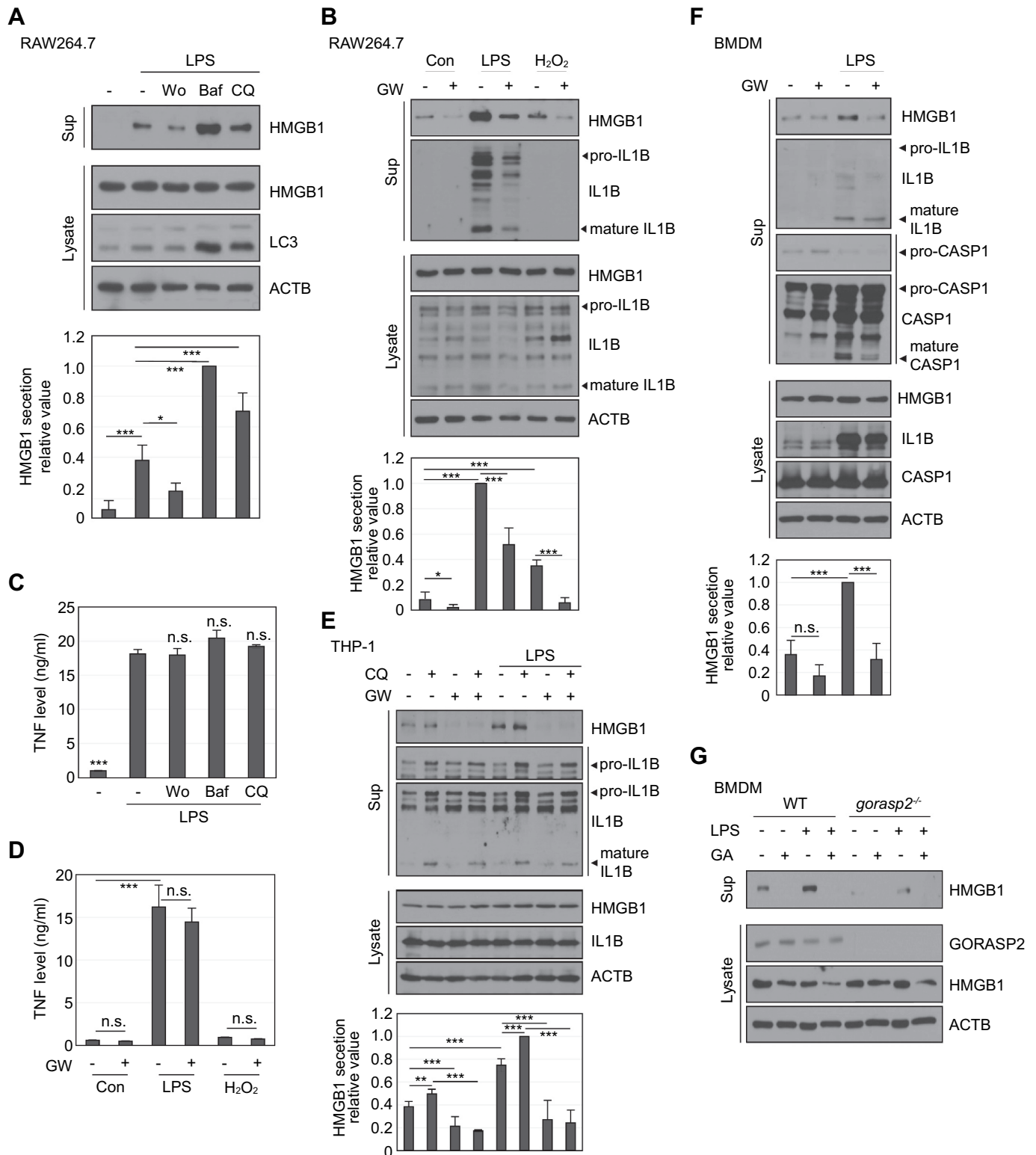 for 2 h, and treated with 250 ng/mL LPS for 24 h. WCLs and supernatants were immunoblotted with anti-HMGB1, anti-LC3, and anti-ACTB antibodies. (B) RAW264.7 cells were pretreated with 2 μM GW (GW4869) for 2 h and treated with 250 ng/mL LPS and 50 μM H_2O_2 for 24 h. WCLs and supernatants were immunoblotted with anti-HMGB1, anti-IL1B, and anti-ACTB antibodies. (C) RAW264.7 cells were pretreated with 100 nM Wo, 20 nM Baf, 20 μM CQ for 2 h, and treated with 250 ng/mL LPS for 24 h. TNF levels were measured in the culture supernatants by ELISA. All results were compared to those of LPS treatment alone. (D) RAW264.7 cells were pretreated with 2 μM GW4869 for 2 h and then treated with 250 ng/mL LPS and 50 μM H_2O_2 for 24 h. TNF level in the supernatants was measured by ELISA. (E) THP-1 cells were pretreated with 2 μM GW4869 for 2 h and treated with 20 μM CQ and 300 ng/mL LPS for 24 h. WCLs and supernatants were immunoblotted with anti-HMGB1, anti-IL1B, and anti-ACTB antibodies. (F) BMDMs were pretreated with 2 μM GW4869 for 2 h, and treated with 250 ng/mL LPS for 24 h. WCLs and supernatants were immunoblotted with anti-HMGB1, anti-IL1B, anti-CASP1, and anti-ACTB antibodies. (G) WT BMDM and gorasp2−/− BMDM cells were pretreated with 0.5 μM GA for 2 h and treated with 250 ng/mL LPS for 24 h. WCLs and culture supernatants were immunoblotted with anti-GORASP2, anti-HMGB1, and anti-ACTB antibodies. Culture supernatants were concentrated with Centricon filters. Data are presented as the mean ± SEM from at least three independent experiments. n.s: not significant, *p < 0.05, **p < 0.01, ***p < 0.001, one-way ANOVA followed by Tukey honestly significant difference posthoc test for multiple comparisons.
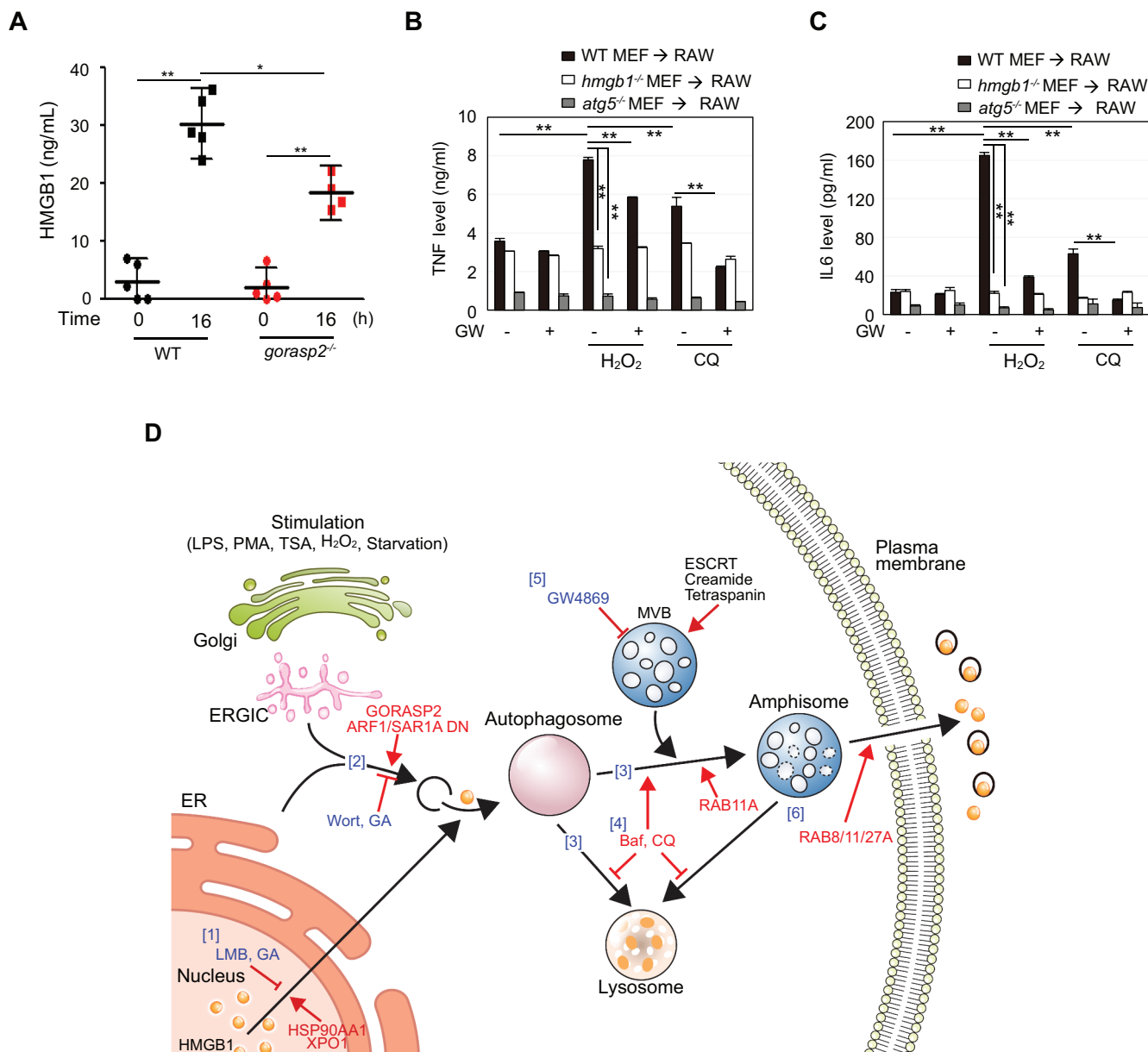
Figure 9. Physiological relevance and proposed model of HMGB1 secretion. (A) WT and *gorasp2*$^{-/-}$ mice were injected intraperitoneally with 2 mg/kg LPS, and blood samples were collected after 16 h. HMGB1 concentration was measured from obtained sera. N = 5 mice per group (one *gorasp2*$^{-/-}$ mouse was dead after LPS injection). Data are presented as the mean ± SEM from at least three independent experiments. *$p < 0.01$, **$p < 0.001$, one-way analysis of variance followed by Tukey honestly significant difference posthoc test for multiple comparisons. (B, C) WT MEF, *hmgb1*$^{-/-}$ MEF, and *atg5*$^{-/-}$ MEF cells were pretreated with 2 μM GW4869 for 2 h and then treated with 50 μM H$_2$O$_2$ and 30 μM CQ for 24 h. The culture supernatants were used to treat RAW264.7 cells at a 1:10 ratio for 6 h. Levels of TNF and IL6 were measured by ELISA. All data are presented as the mean ± SEM from at least three independent experiments. **$p < 0.001$, one-way ANOVA followed by Tukey honestly significant difference posthoc test for multiple comparisons. (D) Model of autophagy machinery and MVB-mediated HMGB1 secretion mechanism. Under normal conditions, HMGB1 resides in the nucleus. Under stress conditions, (1) HMGB1 is transferred by HSP90AA1 and XPO1 from the nucleus to the cytoplasm. (2) Autophagy machinery induced by GORASP2, ARF1^{T39N}, and SAR1A^{Q71L} is engulfed cytosolic HMGB1 into phagophore. (3) Completely closed autophagosome is fused on lysosome (degradation) or MVB (secretion). (4) Under the blockade of autophagosome and lysosome fusion, HMGB1 secretion is elevated via an MVB-dependent pathway. (5) MVB formation is blocked, and HMGB1 secretion is diminished. (6) RAB8A, RAB11A, or RAB27A-mediated vesicle trafficking regulates HMGB1 secretion. Autophagy-based unconventional secretory pathway for extracellular delivery could be observed for IL1B and IL18 [17], supporting this model.

vesicle-coated protein complexes COP I and II, respectively, are small G proteins that play a critical role in conventional ER-to-Golgi trafficking. The blockade of ER-to-Golgi trafficking by dominant inhibitory forms of SAR1A and ARF1 mutants, which induce ER stress and the unfolded protein response, has also been shown to evoke unconventional cell-surface trafficking of CFTR (cystic fibrosis transmembrane conductance regulator) and SLC26A4/pendrin [36–39]. We next investigated the effect of SAR1A and ARF1 DN (dominant-negative) mutants (SAR1A^{T39N} and ARF1^{Q71L}) on HMGB1 secretion. HMGB1 secretion was increased by over-expression of either SAR1A^{T39N} or ARF1^{Q71L} (Figure 6 (A-D)), which was inhibited by GA treatment (Figure 6D). To determine the role of SAR1A and ARF1 DN mutants in

HMGB1 secretion, we tested whether HMGB1 secretion induced by SAR1A and ARF1 DN mutants depends on the autophagy-based UCPS pathway. LC3-II level was more increased by CQ treatment when SAR1A^{T39N} or ARF1^{Q71L} was overexpressed (Figure 6E). HMGB1 secretion by SAR1A^{T39N} and ARF1^{Q71L} overexpression was suppressed by Wort treatment but enhanced by Baf and CQ treatments (Figure 6(E-G)), indicating that SAR1A^{T39N} and ARF1^{Q71L} enhance HMGB1 secretion in an autophagy-dependent manner.

MVB formation regulates HMGB1 secretion

MVBs are a type of late endosome containing unique membrane-enclosed structures with intraluminal vesicles. MVBs are involved in various functions, such as receptor internalization, protein secretion, and lysosomal degradation [40]. Protein secretion regulated by the autophagy machinery involves specific vesicles (amphisome) fused on MVBs and autophagosomes [41]. We hypothesized that HMGB1 is secreted via an MVB-dependent pathway. MVB formation involves two types of machinery; ESCRT protein complex-dependent and ESCRT-independent machinery, also known as ceramide-dependent machinery. To investigate whether the ESCRT protein complex influences HMGB1 secretion, short hairpin RNAs (shRNAs) against ESCRT-related genes (HGS and TSG101) were transiently overexpressed in HEK293T cells to observe HMGB1 secretion. HMGB1 secretion was reduced by shHGS and shTSG101 upon CQ, PMA, TSA, and EBSS treatment (Figure 7A). Following treatment in HEK293 cells with GW4869, which is a SMPD3/nSMase2 (sphingomyelin phosphodiesterase 3) inhibitor used to inhibit ceramide-dependent MVB formation [42,43], HMGB1 secretion was decreased under PMA, TSA, starvation, Baf, and CQ treatments (Figure 7(B,C)). HMGB1 secretion induced by HSP90AA1, GORASP2, and ARF1^{Q71L} overexpression was decreased by GW4869 treatment (Figure 7(D,E)). These results indicate that HMGB1 secretion is regulated by ESCRT and a ceramide-dependent MVB secretion pathway.

RAB proteins play critical roles in vesicular trafficking and membrane fusion, including in autophagy. RAB8A and RAB27A participate in ANXA2 (annexin A2) exophagy [44]. RAB7A is involved in MVB and lysosome fusion, and RAB11A and RAB27A are known to induce components involved in exosome secretion [40,45–47]. Knockdown of each of RAB8A, RAB11A, and RAB27A in HEK293T cells dramatically decreased HMGB1 secretion upon CQ treatment, but RAB7A knockdown did not (Figure 7F).

Autophagy machinery and MVB formation induce HMGB1 secretion in macrophages

Our data showed that HMGB1 secretion is regulated by autophagy machinery and MVB formation in HEK293T cells. When we tested HMGB1 secretion using the RAW264.7 macrophage cell line, HMGB1 secretion was decreased by pre-treatment with Wort but increased by pre-treatment with Baf and CQ under LPS stimulation (Figure 8A). GW4869 decreased HMGB1 secretion under LPS and H_2O_2 treatment

(Figure 8B and S6). In contrast, the level of TNF (tumor necrosis factor), which is secreted via the conventional secretion pathway, showed no significant difference following treatment with the different autophagy inhibitors (Wort, Baf, and CQ) and GW4869 (Figure 8(C,D)). IL1B, a representative unconventional secreted protein, showed a similar secretion pattern as HMGB1 (Figure 8B). The human macrophage cell line THP-1 showed similar secretion patterns for HMGB1 and IL1B following CQ and GW4869 treatments (Figure 8E). BMDM cells also showed decreased HMGB1 secretion following GW4869 treatment (Figure 8F). Additionally, GORASP2-deficient mouse BMDMs showed reduced HMGB1 secretion upon LPS treatment (Figure 8G). Treatments used in our study did not significantly affect cell death when treated to immune cells (Fig. S7). These data demonstrate that HMGB1 secretion is regulated by the autophagy machinery and MVB formation.

Physiological relevance and proposed model of HMGB1 secretion

We examined the role of GORASP2-autophagy-dependent HMGB1 secretion in vivo. C57BL/6 WT and gorasp2$^{-/-}$ mice were injected intraperitoneally with a sublethal dose of LPS (2 mg/kg). Blood samples were collected at 16 h, and HMGB1 concentration in serum was measured. The HMGB1 secretion level was significantly decreased in gorasp2$^{-/-}$ mice compared to that in WT mice after LPS injection (Figure 9A).

To test whether HMGB1 secreted by the GORASP2-autophagy machinery and MVB-mediated pathway regulates inflammation, the culture supernatants from WT MEF, hmgb1$^{-/-}$ MEF, and atg5$^{-/-}$ MEF cells, which were treated with H_2O_2 or CQ in the presence or absence of GW4869, were harvested and used to treat RAW264.7 cells for TNF and IL6 production. Levels of TNF and IL6 were significantly decreased upon treatment with supernatants from hmgb1$^{-/-}$ MEF or atg5$^{-/-}$ MEF cells (Figure 9(B,C)).

In summary, we propose a model of HMGB1 secretion mediated by HSP90AA1, GORASP2, the autophagy machinery, and MVB (Figure 9D). Nuclear HMGB1 is translocated to the cytoplasm by HSP90AA1 and XPO1. Furthermore, post-translational modifications of HMGB1, such as oxidation, helps its binding to XPO1 [27,48]. Cytoplasmic HMGB1 activates autophagy [48–50], and this autophagy activation induces the extracellular secretion of HMGB1. The autophagy machinery ATG5, ATG7, ATG12, and ATG14, and GORASP2 are involved in the packaging of cytosolic HMGB1 into phagophores. When the fusion of autophagosomes and lysosomes is blocked, HMGB1 secretion is increased through the MVB-dependent secretion pathway. RAB8A-, RAB11A-, or RAB27A-mediated vesicle trafficking regulates HMGB1 secretion. The pro-inflammatory cytokines IL1B and IL18 also lack signal peptides and are secreted through an unconventional secretion pathway after inflammasome activation [51,52]. IL1B and IL18 are secreted by the GORASP2-dependent autophagy pathway [17,18].

Discussion

Understanding the mechanism of HMGB1 secretion is crucial since extracellular HMGB1 plays pro-inflammatory functions as a danger-associated molecular pattern molecule, including regulation of cell proliferation, tissue remodeling, and cancer progression [3,4]. Several active secretion mechanisms of HMGB1 have been reported, including those mediated by secretory lysosomes and autophagy. ATG5, ATG7, and ATG12 regulate HMGB1 secretion [6,17]. Moreover, HMGB1 post-translational modifications, including acetylation, methylation, are involved in the secretion [8,12]. We previously reported that HMGB1 phosphorylation, *N*-glycosylation, and intramolecular disulfide bond formation between C23 and C45 play critical roles in HMGB1 nucleo-cytoplasmic transport and secretion [7,9,27]. HMGB1 lacks an ER-targeting peptide sequence; thus, it requires the unconventional secretion pathway as an ER-Golgi -independent route of secretion involving vesicular trafficking. Many proteins, such as DBI/ACBP/AcbA (diazepam binding inhibitor, acyl-CoA binding protein), IL1B, CFTRΔF508, and ANXA2, which are known to be secreted via an unconventional secretion pathway, utilize autophagy components for their secretion [17,39,44,53,54].

In this study, we demonstrated, for the first time, that HMGB1 secretion is regulated by HSP90AA1 and a GORASP2-mediated autophagy-based secretion machinery and the formation of MVBs. HMGB1 is mainly located in the nucleus, and HSP90AA1-dependent trafficking is involved in nucleo-cytoplasmic translocation of HMGB1. Overexpressed HSP90AA1 binds to nuclear HMGB1, resulting in XPO1-mediated nucleo-cytoplasmic export of HMGB1. HSP90AA1 plays important roles in nuclear import or export of cargo proteins. In a study of AGO1 (argonaute RISC component 1), a silencing effector protein in plants, HSP90AA1 was found to bind to AGO1 in the nucleus and induce nucleo-cytoplasmic shuttling via XPO1 [55], which is similar to HMGB1 translocation. However, the mineralocorticoid receptor, a member of the steroid receptor superfamily, is imported into the nucleus in complex with HSP90AA1 [56]. Interestingly, HSP90AA1 facilitates the translocation of cargo proteins in both directions across the nuclear membrane. HSPA7 migrates to the nucleus under cell stress caused by H_2O_2 and interacts with HMGB1 to inhibit the cytoplasmic translocation of HMGB1 [26]. The HSP90AA1 and HSPA7 chaperones bind to each other and function synergistically in protein remodeling [57]. Further studies on how HSP90AA1 leads HMGB1 to expose the nuclear export signal to bind XPO1 by interaction with HMGB1 are necessary.

When HMGB1 is translocated into the cytoplasm, the autophagy machinery and vesicular trafficking are required for HMGB1 secretion. HSP90AA1 enhances the autophagy machinery and vesicular trafficking secretion, similarly to IL1B secretion [17,24,58]. *atg5⁻/⁻* MEF cells showed significant inhibition of HMGB1 secretion even under starvation stress, confirming that HMGB1 is contained in autophagosomes. Baf and CQ treatments to inhibit autolysosome formation promoted HMGB1 secretion. These results suggest that autophagosome formation is important in HMGB1 secretion. *GORASP2* deficiency and SAR1A^T39N and ARF1^Q71L DN mutants inhibited ER-to-Golgi vesicular trafficking and increased autophagosome

formation, resulting in UCPS [36,37,39] and HMGB1 secretion. In patients with cystic fibrosis, CFTRΔF508 (a cystic fibrosis transmembrane conductance regulator mutant containing a phenylalanine deletion at position 508), which is the most common mutant form of CFTR, was transported to the cell membrane via an unconventional secretion pathway during cellular stress [36,37,39]. These findings could suggest that UCPS of not only transmembrane proteins, such as the CFTRΔF508 mutant but also cytosolic proteins, including HMGB1, is increased by autophagosome formation increased by blocking the conventional ER-to-Golgi secretion pathway.

In this regard, an interesting finding is that the type III UCPS of HMGB1 secretion exhibits some similarities to the type IV UCPS of CFTR and SLC26A4. The present study demonstrates that ER-to-Golgi blockade by SAR1A and ARF1 mutants, early autophagy components, and RAB8A are involved in the UCPS of HMGB1 and are also known to play a role in the UCPS of CFTR and SLC26A4 [59]. In contrast, in the case of HSP proteins, there are also some discrepancies between the type III and type IV UCPS pathways. While HSP90AA1 is involved in the type III UCPS of IL1B and HMGB1, HSPA8/HSC70 plays a critical role in the type IV UCPS of CFTR and SLC26A4 [37]. Therefore, it appears that both type III and IV vesicular UCPS pathways share conventional machinery after a certain step, although initial cargo requirements mediated by HSPs are differently achieved.

In exosome biogenesis, autophagy machinery contributes to exosome biogenesis. The ATG12–ATG5-ATG16L1 complex localizes to MVBs and mediates the non-canonical lipidation of LC3B. The ATG5-ATG16L1 complex also facilitates the dissociation of V-ATPase, preventing the acidification of MVBs and their subsequent lysosomal degradation [60]. In our study, inhibition of RAB11 and RAB8A or RAB27A reduced HMGB1 secretion. RAB11 is involved in the formation of amphisomes, which are autophagic vacuoles obtained upon the fusion of MVBs and autophagosomes, and both RAB8A and RAB27A help amphisomes fuse with the plasma membrane. The formation of amphisomes by the fusion of autophagosomes and MVBs is an important step in HMGB1 secretion. Inhibition of ESCRT prevented HMGB1 secretion, and treatment with GW4869, which inhibits ceramide-dependent MVB formation, prevented the extracellular secretion of HMGB1, supporting this mechanism. However, how the fate of proteins is determined by distinguishing between degradative- and secretory autophagy using the same autophagy machinery remains unclear.

HMGB1 secretion is closely related to not only inflammatory diseases but also to various other diseases, including cancer, ischemia-reperfusion injury, Alzheimer's disease, and heart failure [61–68]. The abovementioned results, thus, contribute to the understanding of the sequential regulation of the HMGB1 secretion pathway, which may be useful for designing inhibitors of HMGB1 secretion for treating conditions, such as sepsis.

Materials and methods

Cell culture and reagents

HEK293T cells (ATCC®, CRL-1573™), BMDMs, murine macrophage RAW264.7 cells (ATCC®, TIB-71™), Tet-off

2358 ⬡ Y. H. KIM ET AL.

inducible *atg5*$^{-/-}$ MEF cells, and *atg14*$^{-/-}$ HCT116 cells [69] were cultured in Dulbecco's modified Eagle's medium (Corning, 10–013-CV). Human monocyte THP-1 cells (ATCC® TIB-202™) were cultured in RPMI1640 supplemented with 10% fetal bovine serum (Corning, 35–015-CV), 100 U/mL penicillin, 100 μg/mL streptomycin, and 2 mM L-glutamine (Gibco™, 10,378,016) at 37°C under 5% CO_2. Mouse BMDMs were supplemented with 20% L929 conditioned media. *atg5*$^{-/-}$ MEFs were maintained with 1 μg/mL doxycycline hyclate (Sigma-Aldrich, D9891). For THP-1 differentiation, the cells were treated with 500 nM PMA for 5 h. For cell starvation, the cells were cultured in the EBSS medium (Welgene, LB002-03). The cells were treated with different concentrations of GA (Sigma-Aldrich, G3381), CQ (Sigma-Aldrich, C6628), Baf (Sigma-Aldrich, B1793), Wort (Sigma-Aldrich, W1628), PMA (Sigma-Aldrich, P1585), TSA (Sigma-Aldrich, T8552), LMB (Sigma-Aldrich, L2913), GW4869 (Sigma-Aldrich, D1692), LPS (*E. coli* O111:B4; Sigma-Aldrich, L5293), and H_2O_2 (Sigma-Aldrich, H1009) to observe HMGB1 secretion.

Mice

C57BL/6 WT and *gorasp2*$^{-/-}$ mice were used [70]. Mice were maintained under pathogen-free conditions and a 12:12 h light-dark cycle. Experiments were performed on randomly-selected, age- and gender-matched, 8- to 12-week-old male mice, according to procedures approved by the Institutional Animal Care and Use Committee of the Yonsei Laboratory Animal Research Center (YLARC, 2018–0293).

Plasmids, cloning, shRNA construct, and transfection

cDNA of *HSP90AA1* was subcloned into the pFlag CMV2 plasmid (Creative Biogene, VET1147). The *HSP90AA1* domain mutants NTD (a.a. 1–271), MD (a.a. 272–629), and CTD (a.a. 630–732) were inserted into the pFlag TOPO plasmid (MGmed, Seoul, Korea, MC02204). Construction of *GORASP2-MYC, MYC-SAR1A*^{T39N}, and *HA-ARF1*^{Q71L} plasmids were described previously [39]. MYC-tagged *HMGB1 WT, A* and *B* boxes, *WT GFP-HMGB1*, and *GFP-HMGB1*^{C23S} were described previously [11]. The cDNA of *HMGB1* was sub-cloned into the pGmC plasmid (kindly provided by Prof. Seung Woo Park, Yonsei University College of Medicine, Seoul) to prepare the *HMGB1-mCherry* plasmid. An HMGB1 C-tail deletion mutant (*HMGB1 ΔC*, a.a. 1–185) was prepared in the pCMV-MYC plasmid (Clontech, 631,604). The cDNA of *MAP1LC3B/LC3B* was sub-cloned into the pEGFP-N1 plasmid (Clontech, 6085–1).

shRNA plasmids of control (SHC001), *HSP90AA1* (TRCN0000315007 and TRCN0000315009), *GORASP2* (TRCN0000129348 and TRCN0000127611), *RAB7A* (TRCN0000229643), *RAB8A* (TRCN0000048216), *RAB11A* (TRCN0000073021), *RAB27A* (TRCN0000005295), and *HGS* (TRCN0000379833), *ATG7* (TRCN0000007584 and TRCN0000007585), *ATG12* (TRCN0000272775 and TRCN0000272776), *ATG14* (TRCN0000144080 and TRCN0000121630), and *TSG101* (TRCN0000315042) produced at the BROAD Institute (Cambridge, MA, USA) were

purchased from Yonsei Genomics Center System Biology Core (Yonsei Univ., Seoul, Korea).

Plasmid transfection was carried out using the lipofectamine 2000 reagent (Invitrogen, 52,887) or the Neon transfection system (Invitrogen, MPK10096) for electroporation, according to the manufacturer's instructions. shRNA was transiently transfected into HEK293T cells using the lipofectamine 2000 reagent.

Western blot analysis and IP

For immunoblotting, the cells were lysed with 1× RIPA buffer (GenDEPOT, R4100-010) containing 150 mM NaCl, 1% Triton X-100 (Sigma-Aldrich, 9002–93-1), 1% deoxycholic acid sodium salt (Sigma-Aldrich, 264,101), 0.1% SDS (Sigma-Aldrich, 152–21-3), 50 mM Tris-HCl, pH 7.5, 2 mM EDTA, and a protease inhibitor cocktail (GenDEPOT, P3100). WCLs were centrifuged at $20,000 \times g$ for 10 min at 4°C. Culture supernatants were concentrated using an Amicon Centricon filtration system (Millipore, UFC501096) after removing cell debris. Protein sample buffer [100 mM Tris-HCl, pH 6.8, 2% SDS, 25% glycerol (Biosesang, G1018), 0.1% bromophenol blue, and 5% beta-mercaptoethanol (Amresco, 0482)] was added to the WCLs followed by heating at 94°C for 5 min, and 20 μg of protein was separated by SDS-PAGE followed by transfer to nitrocellulose membranes (GE healthcare, 10,600,001) for immunoblotting. The membranes were blocked with Tris-buffered saline (TBS; 150 mM KCl, 50 mM Tris, 1 mM EDTA, pH 7.4) supplemented with 0.1% Tween 20 (VWR Life Science, 0777), and 5% skim milk (BD Difco, 232,100) for 1 h. Anti-HMGB1 (Abcam, ab18256), anti-GORASP2 (Abcam, ab68713), anti-HSP90 (Abcam, ab13492), anti-XPO1/CRM1 (Santa Cruz Biotechnology, SC-5595), anti-GFP (Santa Cruz Biotechnology, SC-8334 and SC-9996), anti-GORASP1/GRASP65 (Santa Cruz Biotechnology, SC-374,423), anti-GAPDH (Abfrontier, YF-MA10022), anti-ACTB/β-actin (Cell Signaling Technology, 4967), anti-MYC/c-Myc (Invitrogen, 13–2500), anti-LC3B (Sigma-Aldrich, L7543), anti-Flag (Sigma-Aldrich, F3165 and F7425), anti-PDCD6IP/Alix (Abcam, ab117600), anti-HGS (Abcam, ab155539), anti-ATG5 (Novus, NB110-53,818), anti-ATG12 (Cell Signaling Technology, #4180), anti-ATG14 (MBL international, PD026), anti-TSG101 (Santa Cruz Biotechnology, SC-7964), anti-CASP1/caspase1 (AdipoGen, AG-20B-0042), and anti-IL1B/IL-1β (R&D Systems, AF-401-NA) antibodies were used. The membranes were washed with TBS-Tween 20 three times for 10 min each and incubated with the proper horseradish peroxidase-conjugated secondary antibody (Jackson ImmunoResearch, 111–035-003 and 111–035-003) for 1 h, and washed three times for 10 min each with TBS-Tween 20. Enhanced chemiluminescent substrate (GenDEPOT, W3651-012) was used for visualization. The membranes were then stripped by submersion in stripping buffer (Biomax, BWS-1000) at room temperature for 20 min under constant shaking.

IP was performed using 15 μL of SureBeads™ Protein G Magnetic Beads (BIO-RAD, 161–4023). The beads were washed three times with PBST buffer using DynaMag™-2 (Invitrogen, 123.21D) and incubated with 1 μg of a specific

antibody for 1 h at RT. The beads were washed three times with PBST, and 300 μg of protein was added to the beads for overnight rotation at 4°C. The samples were washed three times with PBST and then mixed with a protein sample buffer, followed by heating at 94°C for 5 min. The proteins were separated by SDS-PAGE.

Immunofluorescence and confocal microscopy

To detect the subcellular localization of HMGB1 under starvation conditions or LMB treatment, HEK293T cells were transfected with *WT GFP-HMGB1* or *GFP-HMGB1^C23S* plasmid with or without *WT HSP90AA1-Flag* or its mutant plasmids (NTD, MD, and CTD) or *GORASP2-MYC* for 48 h. The cells were pretreated with 0.5 μM GA for 2 h and incubated with EBSS for 6 h or treated with 20 ng/mL LMB for 24 h in HEK293T cells. Cells were washed with cold PBS, fixed with 4% paraformaldehyde-PHEM buffer (Biosesang, PC2031-100-00) for 30 min at room temperature, and then washed with cold PBS.

To observe HMGB1 and LC3 co-localization upon HSP90AA1 and GORASP2 overexpression, HEK293T cells were transfected with *HMGB1-mCherry, GFP-LC3,* and *GORASP2-MYC* or *HSP90AA1-Flag* and incubated for 48 h. Cells were treated with 20 μM CQ under EBSS for 4 h. After washing with cold PBS, the cells were treated with 20 μg/mL digitonin (Millipore, 300,410) on ice for 5 min to remove cytosolic protein. The cells were immediately washed with cold PBS, fixed with 4% paraformaldehyde-PHEM buffer for 30 min at room temperature, and washed with cold PBS.

For cell permeabilization, the cells were washed with PBS containing 1% Triton X-100 for 10 min, followed by washing with PBS containing 0.02% Tween 20 for 5 min. To block nonspecific antibody binding, the cells were treated with PBS containing 0.02% Tween 20 and 1% bovine serum albumin (BSA) for 5 min. The cells were incubated in PBS containing 3% BSA and anti-Flag and anti-MYC antibodies overnight at 4°C in a humidified chamber. The cells were removed from the solution and washed with 1% BSA in PBST (0.02% Tween) for 5 min. The cells were then incubated with Alexa Fluor 405- and Alexa Fluor 594-conjugated secondary antibodies (Invitrogen, A31553 and A32740) in the dark for 1 h at 37°C. The cells were finally washed with PBST and mounted with or without 4 or 6′-diamidino-2-phenylindole (DAPI; Vectashield, H-1200 and H-1000), and the fluorescence of the cells was measured using a confocal FV1000 microscope (Olympus).

PLA

To observe the interaction between HMGB1 and HSP90AA1 in cells, *MYC-HMGB1* and *HSP90AA1-Flag* were transfected into HEK293T cells on LabTek chamber slides (Nunc, C6807). After 48 h of incubation, the cells were incubated in starvation media for 4 h and fixed with 4% paraformaldehyde-PHEM buffer for 30 min at room temperature. The cells were sequentially washed with 1% Triton X-100, 0.02% Tween 20, and 0.02% Tween 20 plus 1% BSA in PBS. The PLA was performed using a Duolink-in-Situ kit (Sigma-Aldrich, DUO92101) following the

manufacturer's instructions. Briefly, the cells were treated with anti-HMGB1, anti-HSP90AA1, anti-MYC, and anti-Flag antibodies overnight at 4°C, followed by washing. The cells were incubated with a PLA probe mixture and ligation solution at 37°C. For signal amplification, the cells were incubated in polymerase solution at 37°C. After staining with DAPI, fluorescence was visualized under a confocal microscope.

ELISA

Polystyrene microplates (Costa, 3590) were coated with recombinant HSP90AA1 (ATGen, ABIN806289) diluted in carbonate-bicarbonate buffer (pH 9.6) at 4°C for 18 h and then washed three times with PBST. The wells were blocked with PBST containing 3% BSA at 37°C for 2 h. Recombinant HMGB1 was serially diluted in 3%-PBST and added to the wells for 1 h at 37°C. After washing, the anti-HMGB1 antibody was added to each well for incubation for 1 h at 37°C. Horseradish peroxidase-conjugated goat anti-rabbit IgG was added for 30 min at 37°C. Next, 3,3,5,5′-tetramethylbenzidine (TMB; Invitrogen, 002023) substrate was added, and the reaction was stopped by adding 3 N HCl. The optical density was read at 450 nm.

To measure TNF production, RAW264.7 cells were pretreated with 100 nM Wort, 20 nM Baf, 25 μM CQ, and 2 μM GW4869 for 2 h and then treated with 250 ng/mL LPS or 50 μM H_2O_2 for 24 h. The mouse TNF level was measured using a mouse TNF ELISA kit (Invitrogen, 88–7324-88).

Mass spectrometry

HEK293T cells were transfected with the *MYC-HMGB1* plasmid and then lysed with 1× RIPA buffer. MYC affinity beads (Biotool, B23401) were used for the affinity-isolation assay at 4°C for 24 h. The samples were washed three times with cold PBS, and then the protein sample buffer was added for incubation at 94°C for 5 min. The samples were separated by SDS-PAGE. The gels were stained by the Coomassie Brilliant Blue staining method, and protein bands of interest were cut from the gel. Nano liquid chromatography-tandem mass spectrometry (MS/MS)–analysis was performed using a nano HPLC system (Agilent Technologies). The nanochip column (Agilent, 150 × 0.075 mm) was used for peptide separation. The mobile phase A for liquid chromatography separation was 0.1% formic acid in deionized water, and the mobile phase B was 0.1% formic acid in acetonitrile (ThermoFisher, 85,174). The chromatography gradient involved a linear increase from 3% B to 40% B in 80 min, 40% B to 60% B in 10 min, 95% B in 10 min, and 3% B in 20 min. The flow rate was maintained at 400 nL/min. Product ion spectra were collected in information-dependent acquisition mode and analyzed by Agilent 6530 Accurate-Mass Q-TOF using continuous cycles of one full scan time-of-flight MS from 350–1200 m/z (1.0 s) plus three product ion scans from 100–1700 m/z (1.5 s). Precursor m/z values were selected, starting with the most intense ion, using a selection quadrupole resolution of 4 Da. The rolling collision energy feature was used, which determines the collision energy based on the precursor value and charge state. The dynamic exclusion time for precursor ion m/z values was 30 s.

EV preparation and proteinase protection assay

EVs were purified according to differential centrifugation protocols, with slight modification [71]. WT BMDM and *gorasp2*$^{-/-}$ BMDM from C57BL/6 were seeded in culture dishes in complete DMEM containing 8% L929 culture supernatant, at approximately 70% confluence. After washing with DPBS (Gibco, A1285801), the cells were incubated in OPTI-MEM^{TM} (Gibco, 31,985,088) with 250 ng/mL LPS for 24 h. In WT MEF and *atg5*$^{-/-}$ MEF cells were washed with DPBS and incubated in EBSS medium for 14 h with 20 nM Baf and 20 μM CQ. The supernatants were harvested and centrifuged at $300 \times g$ for 10 min to remove the cell debris. The supernatants were centrifuged at $2,000 \times g$ for 20 min to remove apoptotic bodies and then at $10,000 \times g$ for 30 min to remove large particles. Finally, the supernatants were ultracentrifuged at $100,000 \times g$ for 2 h, and the pellets (EVs) were resuspended in DPBS. Protein concentration was measured using the BCA protein assay kit (Thermo Fisher Scientific, 23,225). The same amount of EVs from each sample was incubated with 20 μg/mL proteinase K (New England BioLabs, P8107S), with or without 1% Triton X-100, for 1 h at 37°C. The reaction was stopped by adding 2× protein sample buffer, and the lysates were immunoblotted.

Cytokine production

WT MEF, *hmgb1*$^{-/-}$ MEF, and *atg5*$^{-/-}$ MEF cells were seeded in 12-well plates in complete DMEM, at approximately 70% confluence. After washing twice with DPBS, the cells were pretreated with or without 2 μM GW4869 for 2 h and then treated with 50 μM H_2O_2 and 30 μM CQ for 24 h in EBSS medium. The culture supernatants were collected, and cell debris was removed by centrifugation. To observe the effect of cytokine production by each culture supernatant, RAW264.7 cells were cultured at a density of 5×10^5 cells/mL in 24-well plates in OPTI-MEM medium and treated with the collected supernatant at a 1:10 ratio for 6 h. Culture supernatants were harvested by centrifugation at $2,000 \times g$ at 4°C. Concentrations of TNF and IL6 were measured using sandwich ELISA (R&D System, DY410, and DY206), according to the manufacture's protocol.

Database searching

The mascot algorithm (Matrix Science) was used to identify peptide sequences present in a protein sequence database. HMGB1 (CAG33144.1), *Homo sapiens* (downloaded 21 September 2016) fixed modification; carbamidomethylated at cysteine residues; variable modification; oxidized at methionine residues; maximum allowed missed cleavage; 2, MS tolerance; 100 ppm, MS/MS tolerance; 0.1 Da. Only peptides resulting from trypsin digests were considered.

Statistical analysis

All data are presented as the mean ± SEM of at least three individual measures. In particular, co-localization of HMGB1 and HSP90AA1 or HMGB1 and LC3 was analyzed using the ImageJ software (NIH) by Manders' coefficients method.

Statistical analyses were performed using one-way analysis of variance with the Tukey honestly significant difference posthoc test for multiple comparisons or two-tailed Student's *t*-test for comparisons between two groups using the GraphPad Prism 5 software (GraphPad Software). Differences were considered statistically significant when $p < 0.05$.

Abbreviations

ARF1: ADP ribosylation factor 1; ATG5: autophagy related 5; Baf: bafilomycin A$_1$; CFTR: cystic fibrosis transmembrane conductance regulator; CQ: chloroquine; DN: dominant-negative; EBSS: Earle's balanced salt solution; ER: endoplasmic reticulum; ESCRT: endosomal sorting complexes required for transport; EV: extracellular vesicle; GA: geldanamycin; GFP: green fluorescent protein; GORASP2/GRASP55: golgi reassembly stacking protein 55; H_2O_2: hydrogen peroxide; HEK: human embryonic kidney; HMGB1: high mobility group box 1 protein; HSP90AA1: heat shock protein 90 alpha family class A member 1; IL1B/IL-1β: interleukin 1 beta; IL6: interleukin 6; IP: immunoprecipitation; LMB: leptomycin B; LPS: lipopolysaccharide; MAP1LC3/LC3: microtubule associated protein 1 light chain 3; MEF: mouse embryonic fibroblast; MVB: multivesicular body; PBS: phosphate-buffered saline; PMA: phorbol 12-myristate 13-acetate; RAB: member RAS oncogene family; SAR1A: secretion associated Ras related GTPase 1A; shRNA: short hairpin RNA; TNF/TNF-α: tumor necrosis factor; TSA: trichostatin A; UCPS: unconventional protein secretion; Wort: wortmannin; WT: wild type; XPO1/CRM1: exportin 1.

ORCID

Young Hun Kim http://orcid.org/0000-0003-2701-232X
Man Sup Kwak http://orcid.org/0000-0002-3989-3016
Bin Lee http://orcid.org/0000-0001-9914-8176
Jae Min Shin http://orcid.org/0000-0002-3825-8440
Sowon Aum http://orcid.org/0000-0002-4235-9121
In Ho Park http://orcid.org/0000-0003-2190-5469
Min Goo Lee http://orcid.org/0000-0001-7436-012X
Jeon-Soo Shin http://orcid.org/0000-0002-8294-3234

References

[1] Lange SS, Mitchell DL, Vasquez KM. High mobility group protein B1 enhances DNA repair and chromatin modification after DNA damage. Proc Natl Acad Sci U S A. 2008 Jul 29;105 (30):10320–10325. PMID:18650382

[2] Giavara S, Kosmidou E, Hande MP, et al. Yeast Nhp6A/B and mammalian Hmgb1 facilitate the maintenance of genome stability. Curr Biol. 2005 Jan 11;15(1):68–72. PMID:15649368

[3] Tang D, Kang R, Zeh HJ 3rd, et al. High-mobility group box 1 and cancer. Biochim Biophys Acta. 2010 Jan-Feb;1799(1–2):131–140. PMID:20123075

[4] Andersson U, Tracey KJ. HMGB1 is a therapeutic target for sterile inflammation and infection. Annu Rev Immunol. 2011;29:139–162. PMID:21219181

[5] Ditsworth D, Zong WX, Thompson CB. Activation of poly(ADP)-ribose polymerase (PARP-1) induces release of the pro-inflammatory mediator HMGB1 from the nucleus. J Biol Chem. 2007 Jun 15;282(24):17845–17854. PMID:17430886.

[6] Thorburn J, Horita H, Redzic J, et al. Autophagy regulates selective HMGB1 release in tumor cells that are destined to die. Cell Death Differ. 2009 Jan;16(1):175–183. PMID:18846108

[7] Oh YJ, Youn JH, Ji Y, et al. HMGB1 is phosphorylated by classical protein kinase C and is secreted by a calcium-dependent mechanism. J Immunol. 2009 May 01;182(9):5800–5809. PMID:19380828

[8] Bonaldi T, Talamo F, Scaffidi P, et al. Monocytic cells hyperacetylate chromatin protein HMGB1 to redirect it towards secretion. Embo J. 2003 Oct 15;22(20):5551–5560. PMID:14532127

[9] Kim YH, Kwak MS, Park JB, et al. N-linked glycosylation plays a crucial role in the secretion of HMGB1. J Cell Sci. 2016 Jan 1;129(1):29–38. PMID:26567221

[10] Lu B, Nakamura T, Inouye K, et al. Novel role of PKR in inflammasome activation and HMGB1 release. Nature. 2012 Aug 30;488 (7413):670–674. PMID:22801494.

[11] Youn JH, Shin JS. Nucleocytoplasmic shuttling of HMGB1 is regulated by phosphorylation that redirects it toward secretion. J Immunol. 2006 Dec 01;177(11):7889–7897. PMID:17114460

[12] Ito I, Fukazawa J, Yoshida M. Post-translational methylation of high mobility group box 1 (HMGB1) causes its cytoplasmic localization in neutrophils. J Biol Chem. 2007 Jun 1;282 (22):16336–16344. PMID:17403684

[13] Qin S, Wang H, Yuan R, et al. Role of HMGB1 in apoptosis-mediated sepsis lethality. J Exp Med. 2006 Jul 10;203 (7):1637–1642. PMID:16818669.

[14] Rabouille C, Malhotra V, Nickel W. Diversity in unconventional protein secretion. J Cell Sci. 2012 Nov 15;125(Pt22):5251–5255. PMID:23377655

[15] Nickel W. The unconventional secretory machinery of fibroblast growth factor 2. Traffic. 2011 Jul;12(7):799–805. PMID:21585635

[16] Keller M, Ruegg A, Werner S, et al. Active caspase-1 is a regulator of unconventional protein secretion. Cell. 2008 Mar 7;132 (5):818–831. PMID:18329368

[17] Dupont N, Jiang S, Pilli M, et al. Autophagy-based unconventional secretory pathway for extracellular delivery of IL-1β. Embo J. 2011 Nov 8;30(23):4701–4711. PMID:22068051

[18] Deretic V, Jiang S, Dupont N. Autophagy intersections with conventional and unconventional secretion in tissue development, remodeling and inflammation. Trends Cell Biol. 2012 Aug;22 (8):397–406. PMID:22677446

[19] Nickel W, Rabouille C. Mechanisms of regulated unconventional protein secretion. Nat Rev Mol Cell Biol. 2009 Feb;10(2):148–155. PMID:19122676

[20] Kinseth MA, Anjard C, Fuller D, et al. Golgi-associated protein GRASP is required for unconventional protein secretion during development. Cell. 2007 Aug 10;130(3):524–534. PMID:17655921

[21] Zhang X, Wang Y. GRASPs in Golgi Structure and Function. Front Cell Dev Biol. 2015;3:84. PMID:26779480

[22] Schopf FH, Biebl MM, Buchner J. The HSP90 chaperone machinery. Nat Rev Mol Cell Biol. 2017 Jun;18(6):345–360. PMID:28429788

[23] Pearl LH, Prodromou C. Structure and mechanism of the Hsp90 molecular chaperone machinery. Annu Rev Biochem. 2006;75:271–294. PMID:16756493

[24] Zhang M, Kenny SJ, Ge L, et al. Translocation of interleukin-1β into a vesicle intermediate in autophagy-mediated secretion. Elife. 2015 Nov 2;4. doi:10.7554/eLife.11205. PMID:26523392.

[25] Bianchi ME. HMGB1 loves company. J Leukoc Biol. 2009 Sep;86 (3):573–576. PMID:19414536

[26] Tang D, Kang R, Xiao W, et al. Nuclear heat shock protein 72 as a negative regulator of oxidative stress (hydrogen peroxide)-induced HMGB1 cytoplasmic translocation and release. J Immunol. 2007 Jun 1;178(11):7376–7384. PMID:17513788

[27] Kwak MS, Kim HS, Lkhamsuren K, et al. Peroxiredoxin-mediated disulfide bond formation is required for nucleocytoplasmic translocation and secretion of HMGB1 in response to inflammatory stimuli. Redox Biol. 2019 Jun;24:101203. PMID:31026770.

[28] Marzook H, Deivendran S, George B, et al. Cytoplasmic translocation of MTA1 coregulator promotes de-repression of SGK1 transcription in hypoxic cancer cells. Oncogene. 2017 Sep 14;36 (37):5263–5273. PMID:28504714.

[29] Falsone SF, Gesslbauer B, Tirk F, et al. A proteomic snapshot of the human heat shock protein 90 interactome. FEBS Lett. 2005 Nov 21;579(28):6350–6354. PMID:16263121.

[30] D'Angelo G, Prencipe L, Iodice L, et al. GRASP65 and GRASP55 sequentially promote the transport of C-terminal valine-bearing cargos to and through the Golgi complex. J Biol Chem. 2009 Dec 11;284(50):34849–34860. PMID:19840934

[31] Tang D, Kang R, Cheh CW, et al. HMGB1 release and redox regulates autophagy and apoptosis in cancer cells. Oncogene. 2010 Sep 23;29(38):5299–5310. PMID:20622903.

[32] Xu C, Liu J, Hsu LC, et al. Functional interaction of heat shock protein 90 and Beclin 1 modulates Toll-like receptor-mediated autophagy. Faseb J. 2011 Aug;25(8):2700–2710. PMID:21543763

[33] Redmann M, Benavides GA, Berryhill TF, et al. Inhibition of autophagy with bafilomycin and chloroquine decreases mitochondrial quality and bioenergetic function in primary neurons. Redox Biol. 2017 Apr;11:73–81. PMID:27889640.

[34] Leidal AM, Huang HH, Marsh T, et al. The LC3-conjugation machinery specifies the loading of RNA-binding proteins into extracellular vesicles. Nat Cell Biol. 2020 Feb;22(2):187–199. PMID:31932738.

[35] Zhong Y, Wang QJ, Li X, et al. Distinct regulation of autophagic activity by Atg14L and Rubicon associated with Beclin 1-phosphatidylinositol-3-kinase complex. Nat Cell Biol. 2009 Apr;11(4):468–476. PMID:19270693

[36] Gee HY, Noh SH, Tang BL, et al. Rescue of DeltaF508-CFTR trafficking via a GRASP-dependent unconventional secretion pathway. Cell. 2011 Sep 2;146(5):746–760. PMID:21884936

[37] Jung J, Kim J, Roh SH, et al. The HSP70 co-chaperone DNAJC14 targets misfolded pendrin for unconventional protein secretion. Nat Commun. 2016 Apr 25;7:11386. PMID:27109633

[38] Kim J, Noh SH, Piao H, et al. Monomerization and ER relocalization of GRASP is a requisite for unconventional secretion of CFTR. Traffic. 2016 Jul;17(7):733–753. PMID:27062250

[39] Noh SH, Gee HY, Kim Y, et al. Specific autophagy and ESCRT components participate in the unconventional secretion of CFTR. Autophagy. 2018;14(10):1761–1778. PMID:29969945

[40] Piper RC, Katzmann DJ. Biogenesis and function of multivesicular bodies. Annu Rev Cell Dev Biol. 2007;23:519–547. PMID:17506697

[41] Giuliani F, Grieve A, Rabouille C. Unconventional secretion: a stress on GRASP. Curr Opin Cell Biol. 2011 Aug;23 (4):498–504. PMID:21571519

[42] Guo BB, Bellingham SA, Hill AF. The neutral sphingomyelinase pathway regulates packaging of the prion protein into exosomes. J Biol Chem. 2015 Feb 6;290(6):3455–3467 . PMID:25505180

[43] Trajkovic K, Hsu C, Chiantia S, et al. Ceramide triggers budding of exosome vesicles into multivesicular endosomes. Science. 2008 Feb 29;319(5867):1244–1247. PMID:18309083

[44] Chen YD, Fang YT, Cheng YL, et al. Exophagy of annexin A2 via RAB11, RAB8A and RAB27A in IFN-γ-stimulated lung epithelial cells. Sci Rep. 2017 Jul 18;7(1):5676. PMID:28720835

[45] Bucci C, Thomsen P, Nicoziani P, et al. Rab7: a key to lysosome biogenesis. Mol Biol Cell. 2000 Feb;11(2):467–480. PMID:10679007

[46] Ostrowski M, Carmo NB, Krumeich S, et al. Rab27a and Rab27b control different steps of the exosome secretion pathway. Nat Cell Biol. 2010 Jan;12(1):19–30. sup pp 11-13. PMID:19966785

[47] Savina A, Fader CM, Damiani MT, et al. Rab11 promotes docking and fusion of multivesicular bodies in a calcium-dependent manner. Traffic. 2005 Feb 6;2:131–143. PMID:15634213

[48] Pan X, Song X, Wang C, et al. H(2)Se induces reductive stress in HepG2 cells and activates cell autophagy by regulating the redox of HMGB1 protein under hypoxia. Theranostics. 2019;9 (6):1794–1808. PMID:31037139

[49] Tang D, Kang R, Livesey KM, et al. High mobility group box 1 (HMGB1) activates an autophagic response to oxidative stress. Antioxid Redox Signal. 2011 Oct 15;15;15(8):2185–2195. PMID:21395369

[50] Tang D, Loze MT, Zeh HJ, et al. The redox protein HMGB1 regulates cell death and survival in cancer treatment. Autophagy. 2010 Nov 6;6(8):1181–1183. PMID:20861675

[51] Bae JH, Jo SI, Kim SJ, et al. Circulating cell-free mtDNA contributes to AIM2 inflammasome-mediated chronic inflammation in patients with Type 2 diabetes. Cells. 2019 Apr 8;8(4):328. PMID:30965677

[52] Arend WP, Palmer G, Gabay C.IL-1, IL-18, and IL-33 families of cytokines. Immunol Rev. 2008 Jun;223:20–38. PMID:18613828.

[53] Bruns C, McCaffery JM, Curwin AJ, et al. Biogenesis of a novel compartment for autophagosome-mediated unconventional protein secretion. J Cell Biol. 2011 Dec 12;195(6):979–992. PMID:22144692

[54] Duran JM, Anjard C, Stefan C, et al. Unconventional secretion of Acb1 is mediated by autophagosomes. J Cell Biol. 2010 Feb 22;188 (4):527–536. PMID:20156967

[55] Bologna NG, Iselin R, Abriata LA, et al. Nucleo-cytosolic shuttling of ARGONAUTE1 prompts a revised model of the plant microRNA pathway. Mol Cell. 2018;69(4):709–719.e705. PMID:29398448

[56] Grossmann C, Ruhs S, Langenbruch L, et al. Nuclear shuttling precedes dimerization in mineralocorticoid receptor signaling. Chem Biol. 2012;19(6):742–751. PMID:22726688

[57] Genest O, Wickner S, Doyle SM. Hsp90 and Hsp70 chaperones: collaborators in protein remodeling. J Biol Chem. 2019;294 (6):2109–2120. PMID:30401745

[58] Iula L, Keitelman IA, Sabbione F, et al. Autophagy mediates interleukin-1β secretion in human neutrophils. Front Immunol. 2018;9:269. PMID:29515581

[59] Gee HY, Kim J, Lee MG. Unconventional secretion of transmembrane proteins. Semin Cell Dev Biol. 2018;83:59–66. PMID:29580969

[60] Xu J, Camfield R, Gorski SM. The interplay between exosomes and autophagy - partners in crime. J Cell Sci. 2018;131(15): jcs215210. PMID:30076239

[61] Takata K, Kitamura Y, Kakimura J, et al. Role of high mobility group protein-1 (HMG1) in amyloid-β homeostasis. Biochem Biophys Res Commun. 2003 Feb 14;301(3):699–703. PMID:12565837.

[62] Taguchi A, Blood DC, Del Toro G, et al. Blockade of RAGE-amphoterin signalling suppresses tumour growth and metastases. Nature. 2000 May 18;405(6784):354–360. PMID:10830965.

[63] Bartling B, Hofmann HS, Weigle B, et al. Down-regulation of the receptor for advanced glycation end-products (RAGE) supports non-small cell lung carcinoma. Carcinogenesis. 2005 Feb;26 (2):293–301. PMID:15539404

[64] Izuishi K, Tsung A, Jeyabalan G, et al. Cutting edge: high-mobility group box 1 preconditioning protects against liver ischemia-reperfusion injury. J Immunol. 2006 Jun 15;176 (12):7154–7158. PMID:16751357.

[65] Davé SH, Tilstra JS, Matsuoka K, et al. Ethyl pyruvate decreases HMGB1 release and ameliorates murine colitis. J Leukoc Biol. 2009 Sep;86(3):633–643. PMID:19454652

[66] Luan ZG, Zhang H, Ma XC, et al. Role of high-mobility group box 1 protein in the pathogenesis of intestinal barrier injury in rats with severe acute pancreatitis. Pancreas. 2010 Mar;39(2):216–223. PMID:19786932

[67] Ding HS, Yang J. High mobility group box-1 and cardiovascular diseases. Saudi Med J. 2010 May;31(5):486–489. PMID:20464035

[68] Volz HC, Seidel C, Laohachewin D, et al. HMGB1: the missing link between diabetes mellitus and heart failure. Basic Res Cardiol. 2010 Nov;105(6):805–820. PMID:20703492.

[69] Woo M, Choi HI, Park SH, et al. The unc-51 like autophagy activating kinase 1-autophagy related 13 complex has distinct functions in tunicamycin-treated cells. Biochem Biophys Res Commun. 2020 Apr 9;524(3):744–749. PMID:32035621.

[70] Kim J, Kim H, Noh SH, et al. Grasp55(-/-) mice display impaired fat absorption and resistance to high-fat diet-induced obesity. Nat Commun. 2020 Mar 17;11(1):1418. PMID:32184397

[71] Théry C, Amigorena S, Raposo G, et al. Isolation and characterization of exosomes from cell culture supernatants and biological fluids. Curr Protoc Cell Biol. 2006 Apr;30:3.22.1–3.22.29. PMID:18228490. Chapter 3: Unit3.22.